SPRINGBACK ANALYSIS IN BENDING THROUGH FINITE ELEMENT METHOD BASED ARTIFICIAL NEURAL NETWORKS

A THESIS SUBMITTED TO
THE GRADUATE SCHOOL OF NATURAL AND APPLIED SCIENCES
OF
MIDDLE EAST TECHNICAL UNIVERSITY

BY

ÖZGÜ ŞENOL

IN PARTIAL FULFILLMENT OF THE REQUIREMENTS
FOR
THE DEGREE OF MASTER OF SCIENCE
IN
MECHANICAL ENGINEERING

SEPTEMBER 2013

Approval of the thesis:

SPRINGBACK ANALYSIS IN BENDING THROUGH FINITE ELEMENT METHOD BASED ARTIFICIAL NEURAL NETWORKS

submitted by **ÖZGÜ ŞENOL** in partial fulfillment of the requirements for the degree of **Master of Science in Mechanical Engineering Department, Middle East Technical University by,**

Prof. Dr. Canan ÖZGEN
Dean, Graduate School of **Natural and Applied Sciences** _____

Prof. Dr. Süha ORAL
Head of Department, **Mechanical Engineering** _____

Prof. Dr. Haluk DARENDELİLER
Supervisor, **Mechanical Engineering Dept., METU** _____

Assist. Prof. Dr. Volkan ESAT
Co-Supervisor, **Mechanical Engineering Program, METU NCC** _____

Examining Committee Members:

Prof. Dr. Mustafa İlhan GÖKLER
Mechanical Engineering Dept., METU _____

Prof. Dr. Haluk DARENDELİLER
Mechanical Engineering Dept., METU _____

Prof. Dr. Levend PARNAS
Mechanical Engineering Dept., METU _____

Assist. Prof. Dr. Volkan ESAT
Mechanical Engineering Program, METU NCC _____

Prof. Dr. Can ÇOĞUN
Mechanical Engineering Dept., Çankaya University _____

Date: 04.09.2013

I hereby declare that all information in this document has been obtained and presented in accordance with academic rules and ethical conduct. I also declare that, as required by these rules and conduct, I have full cited and referenced all material and results that are not original to this work.

Name, Last name : Özgü ŞENOL

Signature :

ABSTRACT

SPRINGBACK ANALYSIS IN BENDING THROUGH FINITE ELEMENT METHOD BASED ARTIFICIAL NEURAL NETWORKS

Şenol, Özgü
M.Sc., Department of Mechanical Engineering
Supervisor: Prof. Dr. Haluk Darendeliler
Co-Supervisor: Assist. Prof. Dr. Volkan Esat
September 2013, 87 pages

Springback prediction is vital in order to obtain the desired part shape in metal forming processes. In most of the applications, springback amount is determined by trial and error procedures, and recently by using numerical methods or through handbook tables. Artificial Neural Network (ANN) is a helpful tool for the engineers and applied in this study to determine the springback amounts in air, V-die and wipe bending processes. For this purpose, bending processes are analyzed by commercial finite element (FE) software and springback amounts are collected for different parameters such as thickness, die radius, bending angle, etc. Then, by developing a feedforward neural network with backpropagation learning algorithm, the springback amounts for bending applications are determined. ANN results of three bending operations are combined to analyze an industrial workpiece. In addition to this, an experimental bending operation is analyzed for air bending process. It is shown that ANN can be effectively applied to determine springback amount in air, V-die and wipe bending.

Keywords: Finite Element Method (FEM), Neural Network, Air Bending, V-die Bending, Wipe Bending

ÖZ

BÜKME İŞLEMLERİNDEKİ GERİ YAYLANMANIN SONLU ELEMANLAR YÖNTEMİNE DAYANAN YAPAY SİNİR AĞLARI İLE ANALİZİ

Şenol, Özgü
Yüksek Lisans, Makina Mühendisliği Bölümü
Tez Yöneticisi: Prof. Dr. Haluk Darendeliler
Ortak Tez Yöneticis: Yrd. Doç. Dr. Volkan Esat
Eylül 2013, 87 sayfa

Metal şekillendirme işlemlerinde istenilen parça şeklinin elde edilebilmesi için geri yaylanmanın belirlenmesi önem taşımaktadır. Geri yaylanma miktarı birçok uygulamada deneme yanılma yöntemi, sayısal metotlar ya da kitaplar aracılığı ile saptanmaktadır. Yapay sinir ağı algoritması mühendisler için faydalı bir araçtır ve bu çalışmada serbest, V-kalıp ve kenar bükmede geri yaylanma miktarının tespitinde kullanılmıştır. Bu amaçla, bükme işlemleri sonlu elemanlar yöntemi ile analiz edilmiş ve kalınlık, kalıp kenar yarıçapı, bükme açısı gibi değişik parametreler için geri yaylanma miktarları bir araya getirilmiştir. Daha sonra, bükme uygulamaları için geri yaylanma miktarları, geri yayılımlı öğrenme algoritmasına sahip bir yapay sinir ağı geliştirilerek saptanmıştır. Üç bükme işleminin yapay sinir ağı sonuçları endüstriyel bir parçanın analizi için birleştirilmiştir. Buna ek olarak serbest bükme işlemi için deneysel bir bükme işlemi analiz edilmiştir. Serbest, V-kalıp ve kenar bükme işlemlerindeki geri yaylanma miktarlarının saptanmasında yapay sinir ağının etkili bir şekilde kullanılabileceği gösterilmiştir.

Anahtar Kelimeler: Sonlu Elemanlar Yöntemi, Sinir Ağı, Serbest Büküm, V-kalıp Büküm, Kenar Büküm

To My Family

ACKNOWLEDGEMENTS

I am grateful to express my gratitude to my thesis supervisors Prof. Dr. Haluk DARENDELİLER and Assist. Prof. Dr. Volkan ESAT for their guidance, endless support and helpful criticism throughout the progress of my thesis study.

I also want to thank Prof. Dr. Mustafa İlhan GÖKLER, Prof. Dr. Levend PARNAS, and Prof. Dr. Can ÇOĞUN for their helpful comments.

I wish to thank the members of the Materials Testing Laboratory of the Department of Mechanical Engineering for the support and the assistance.

I am also grateful to the members of the General Workshops Directorate for their support and help which made a valuable contribution to my thesis.

The special thanks go to my family for their never ending love, support, guidance, and tolerance.

TABLE OF CONTENTS

LIST OF TABLES

TABLES

LIST OF FIGURES

FIGURES

LIST OF SYMBOLS

α	Bend angle
λ	Levenberg's damping factor
δ	Weight update vector
υ	Poisson's ratio
E	Elastic modulus
I	Identity matrix
K	Springback factor
J	Jacobian's matrix
R	Radius
R_i	Initial radius
R_f	Final radius
W:	Width
t:	Thickness

CHAPTER 1

INTRODUCTION

1.1 Motivation

Bending is a frequently employed manufacturing process in modern industry. Sheet metal bending is one of the widely used bending processes and embodies important manufacturing considerations. After bending operation, metals show a tendency to partially return to their original shape due to elastic recovery of the material. The reason for elastic recovery, which is also called springback, is elastic stresses about the neutral axis. In sheet metal forming, springback is an important issue which can lead to crucial problems during component assembly, if not considered and compensated for. Large number of studies is being done to compensate for springback in bending and sheet metal forming.

1.2 Bending

Bending of sheet metals can be defined as the straining of metal around a straight axis. The metal on the inside of the neutral plane is compressed, while the metal on the outside is stretched during the bending process as shown in Figure 1.1 [1]. Sheet metal is stressed beyond the yield strength after bending, the sheet metal is deformed plastically and has a permanent shape.

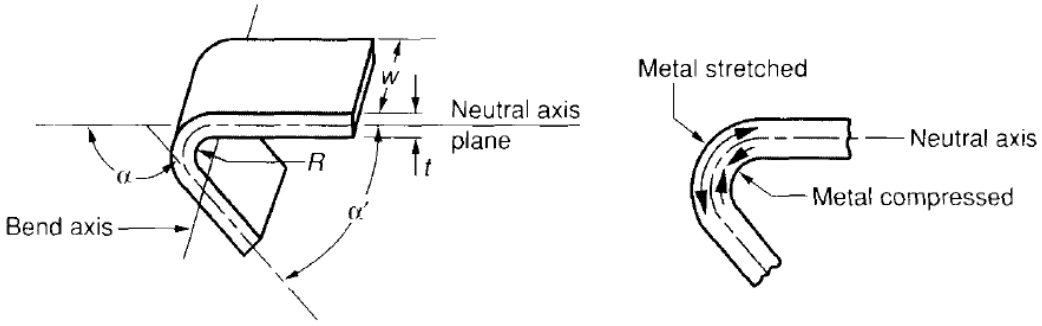

Figure 1.1 Terminology in bending

Distance of the neutral axis from the inside of the bend is 0.3t to 0.5t generally, where t is the thickness of the sheet as shown in Figure 1.1.There are some crucial parameters which influence the bending operations such as bend angle, α, and bend radius, R. When bend radius decreases, strain in the bent material increases. Mechanical properties of the material and its thickness determine minimum bend radius. For bending operations in which bend

angles are over 90°, some problems may arise as the bend angle becomes larger. In this case, the value of bend radius becomes more critical and the material hardness plays a more important role in the success of the bending process [2].

1.3 Bending Types

Wipe-bending, air (free) bending, v-die bending, swivel bending, hemming, curling, and seaming are frequently used sheet metal forming. In this thesis, air, V-die, and wipe bending are investigated.

1.3.1 Wipe-bending

Wipe-bending processes are frequently used in industry especially to produce flanges. Wipe-bending is also known as flanging. If the bent flange is relatively shorter than the remaining part of the sheet, this type of bending may be preferred [2]. Die, punch, blank holder and sheet metal are the components in wipe-bending as shown in Figure 1.2 [5]. The sheet is clamped between the die and blank holder first, and then the punch moves towards the workpiece vertically downwards to bend it. As soon as the workpiece is fully bent, the punch moves upwards rapidly.

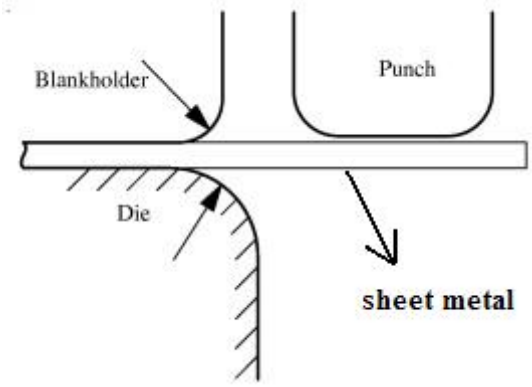

Figure 1.2 Wipe-bending [5]

1.3.2 Air (free) bending

In air bending process, necessary bending angle is obtained with the help of a die and a punch with a couple of shoulders (Figure 1.3). The die gap is set according to the process requirements, and the sheet metal is supported on the shoulders of the die on both sides. The punch at the midpoint of the die is given a displacement, and the die is deep enough to avoid the sheet from striking its bottom [6]. Three-point contact of metal occurs in air bending through punch tip and die edges. Most bend allowance formulae are based on air bending process. To obtain different bending angles in air bending, there is no need to change any equipment or dies as the punch stroke determines the bend angles. To obtain the desired

bend angle, accurate control of the punch stroke is necessary. In air bending, forming forces are relatively small.

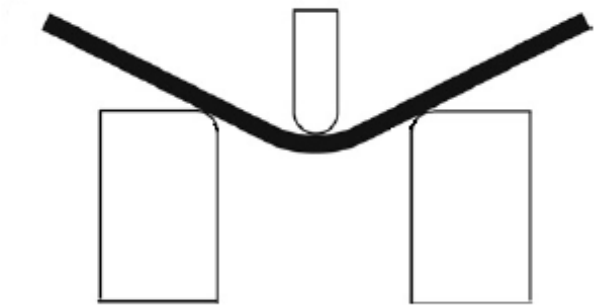

Figure 1.3 Air (free) bending [7]

1.3.3 V-die bending

In V-die bending process, sheet metal is bent in a single die. Different phases of the V-die bending are illustrated in Figure 1.4. The sheet metal is bent between a V-shaped die and punch. During V-die bending, the workpiece is bent with the help of the force acting on the punch. On the outer and inner surfaces, this plastic deformation starts directly underneath the punch. On the outer surface maximum tensile stress is observed whereas on the inner surface maximum compressive stress is seen. The initial bending stage of the V-die bending is similar to air bending as it starts as soon as the punch contacts the workpiece. Unlike air bending, process continues until the workpiece's legs become tangential to the faces of the die [8].

In V-die bending, just before the fully loaded stage of the process, the two end regions of the bent-up workpiece leave the die and rest on the punch. The ends of the sheet are bent towards the die again as the punch continuous to move downwards and on both sides secondary bent-up regions are generated just above the main bent-up region. The sheet is fully supported by the die and the punch at the fully loaded state. The secondary bent-up regions cause springback in the opposite direction to the springback resulted by the main bent-up region after the sheet is removed from the die and the punch [2]. In V-die bending, the clearance between the punch and the die is the thickness of the workpiece. In the V-die bending process, the usual thickness of the workpiece is between 0.5 mm and 25 mm. Several types of V-die bending process are shown in Figure 1.5.

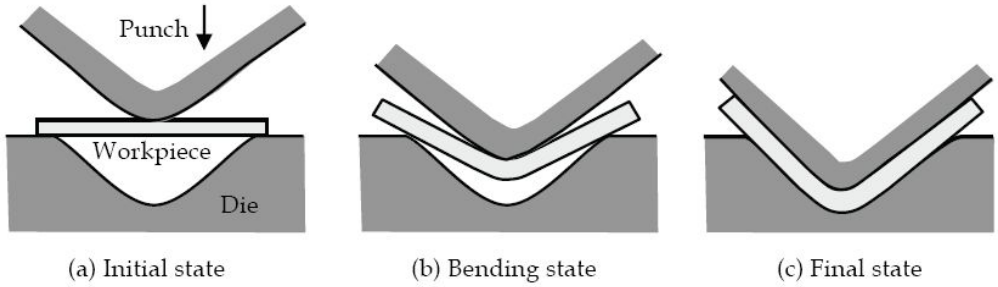

Figure 1.4 Different phases of the V-die bending [8]

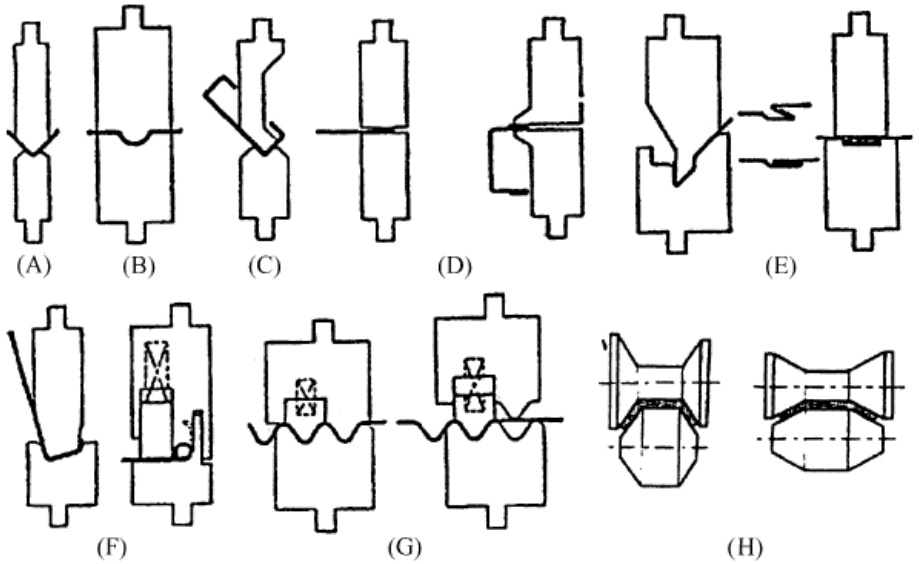

Figure 1.5 Several types of V-die bending process [9]

1.4 Springback

Upon release of the forming force, metals show a tendency to partially return to their original shape due to elastic recovery of the material. The reason for elastic recovery, which is also called springback, is elastic stresses about the neutral axis. In sheet metal forming, springback is an important issue which can lead to important problems during component assembly, if not considered thoroughly. Springback is affected mainly by two factors; mechanical properties and geometric properties. Material's mechanical properties influencing springback are mainly modulus of elasticity, yield strength, strain hardening characteristics, and Poisson's ratio. Some of the essential geometric properties affecting springback are sheet thickness, tooling geometry, and clearance between punch and die or workpiece.

To define springback numerically, K, springback factor is used. Related parameters with springback are initial radius R_i, final radius R_f, part angle α_f, die or bend angle α_i, and sheet thickness t, which are illustrated in Figure 1.6.

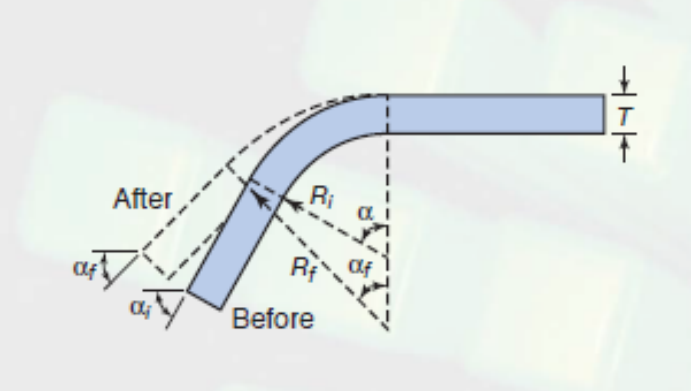

Figure 1.6 Springback parameters [10]

During the process, it is assumed that the arc length on the neutral axis, W, remains unchanged in the bent-up region of the workpiece. The relationship between arc length, *W*, R_i, R_f, α_f, α_i is [2]:

$$W = a_f (R_i + \frac{t}{2}) = a_i (R_f + \frac{t}{2}) \tag{1.1}$$

The springback factor, K, is defined as [2]:

$$K = a_i / a_f = (R_i + \frac{t}{2}) / (R_f + \frac{t}{2}) \tag{1.2}$$

In all of the bending processes, it is virtually impossible to have zero springback and therefore it must be taken into account in every bending process. Higher bend angle and smaller bend radius are used in bending processes to compensate for springback, however variations in the process parameters and material properties affect spring-back dramatically. This implies that springback is almost inevitable.

1.5 Artificial Neural Network

An artificial neural network (ANN) is a system based on the operation of biological neural networks. ANN attempts to imitate the learning activities of the human brain. Artificial neural networks are made of interconnecting artificial neurons which may share some properties of biological neurons. Neural networks learn by example like people. Neural

networks possess the ability to model input-output relationship of data in a nonlinear fashion. Neural networks have been used in a broad range of applications including pattern classification, pattern recognition, optimization, prediction and automatic control.
Generally multi-layer neural network is used in the systems. A multi-layer neural network consists of an input layer, hidden layers and an output layer. The first layer is the input layer and it accepts the input data for training. Input layer consists of a number of neurons usually equal to the number of input. Hidden layers are between the input and output layer. Hidden layer receives the data from the input layer, then processes the data and finally sends a response to the output layer. Hidden layer consists of many computational neurons and transfer functions. Output layer consists of a number of computational neurons. Figure 1.7 shows a general structure of the artificial neural networks.

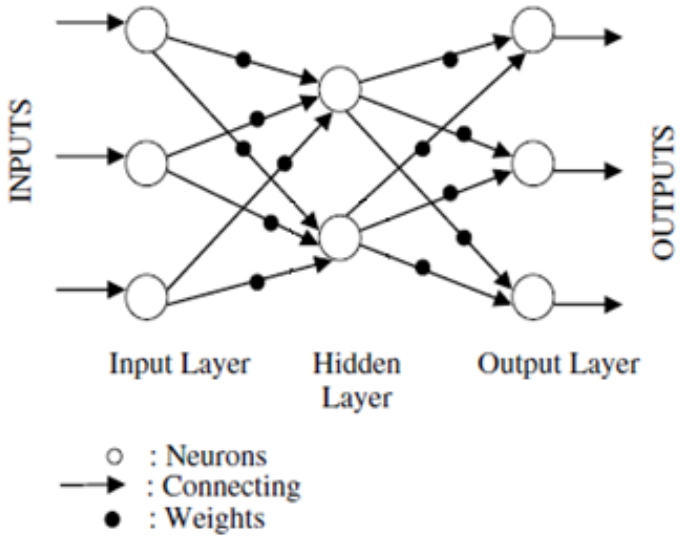

Figure 1.7 General structure of Artificial Neural Network [5]

Neural networks can be divided into two main classes in terms of pattern of connections. These two main classes are feedforward neural networks and recurrent neural networks. There are three types of learning algorithms widely-used in neural networks, which are supervised learning (error based), reinforced learning, and unsupervised learning.

1.6 Scope of the Thesis

In this study, several bending operations, namely wipe bending, air (free) bending and V-die bending are modeled, simulated and analyzed to investigate the effects of springback. An artificial neural network structure is then designed for each bending process to employ in future analysis of bending operations and springback predictions.

To model the bending processes, commercial finite element software MSC. MARC/MENTAT and to design ANN structure commercial mathematical modeling software MATLAB are used. In the finite element modeling, four different material models are used for each bending process and effects of different sheet thicknesses, different punch and die radii on springback are investigated. For future springback prediction ANN algorithm is designed and used. ANN predictions are compared with FEA results.
Finite element models and ANN models for wipe, air and V-die bending processes are combined to investigate springback in a complicated commercial product and the results are discussed.

In experimental analysis several stainless steel (SS304) sheets are used in air bending process with two different thickness values. After experimental and finite element analyses of the parts, results are compared and the effects of material properties, bending angle and geometric properties of the sheets are discussed.

CHAPTER 2

LITERATURE SURVEY

Several researchers have worked on the effects of springback phenomenon in various forming operations. Gardiner [11] studied on springback in pure bending of metals and he achieved an analytical solution for this phenomenon with perfect elastoplasticity. Panthi et al. [12] modeled sheet metal bending process with a large deformation algorithm based on Total – Elastic – Incremental - Plastic Strain. They examined the effect of load on springback for different sheet thicknesses and different die radii. Lee and Yang [13] used the Taguchi method to evaluate the numerical factors influencing springback. They chose U-draw bending process as an evaluation problem due to its large springback. Yi et al. [14] claimed that FE models are not successful to predict springback and they derived a model to predict the springback analytically for six different deformation patterns by using differential strains after relief from the maximum bending stress. Pahole et al. [15] researched bending of sheet metal for angles greater than 90 degrees with simple forming tools. They claimed that for complicated bends, bending method “traktrix” (in two steps) or the method “turning of the strip” (in one step) can be used. For bending process they used the principle of “traktrix“curve known in field of deep drawing process. They developed “traktrix” curve for more complicated bends. Marretta et al. [16] aimed to develop a design tool for stamping processes. S-shaped U-channel stamping operation carried out on a lightweight aluminum alloy of automotive interest is investigated in their study. They especially focused on the control of springback phenomena and the prevention of excessive part thinning. They proposed an approach which is multi-objective optimization problem. This approach is a combination of Response Surface Methodology (RSM), Monte Carlo Simulation (MCS) method and finite element (FEM) numerical simulation. Hsu and Shien [17] used elastic-plastic finite element approach is based on the flow rule associated with Hill's quadratic yield criterion to simulate and analyze axisymmetric sheet metal forming processes punch stretching and deep drawing. They obtained numerical solutions to simulate the springback effect in various sheet metal forming operations from a total Lagrangian formulation of a finite-strain thin shell theory. They compared the calculated results with experimental data and existing numerical solutions. Esat et al. [18] calculated the amount of springback, the total equivalent plastic strain and the equivalent Von Mises stress distributions of different aluminum materials with different thicknesses in bending operations by commercially available finite element analysis (FEA) software. They compared the FEA results with empirical data. Meinders et al. [19] provided guidelines regarding the mesh discretization and a new through-thickness integration scheme for shell elements to improve the springback prediction by FE analysis. An industrial automotive part is used to apply the procedure to automatically compensate the tool geometry, including the CAD description.

Various researchers have worked on finite element analysis and simulation of V-die bending. They researched the effects of springback phenomenon particularly. Tekiner [9] carried out an experimental study on determination of springback of bent products. With different bend

angles, the amounts of springback of several sheet metals were achieved on a modular V bending die. Springback graph were produced for six different materials in 18 different modular dies by using four different bending methods. Huang et al. [20] offered a model based on the tensile properties of the material and the geometry of the tools used. Their model predicts the correct punch load for bending, and the precise final shape of products after unloading. They provided an elasto-plastic incremental finite-element computer code to simulate the V-die bending of sheet metal. Tekaslan et al. [21] researched the subject of bending dies and springback in bending process. They aimed to find out how much steel sheet metal materials can be bent without failure in various angles and to find springback in V-die bending. They prepared 15 different dies, they bent more than 150 samples and they measured the obtained angles with profile meter. Chan et al. [22] studied a different type of V-die bending model within a forming process with one clamped end and one free end. They investigated the effects of different punch radii, punch angles and die-lip radii as well as the effect of the punch displacement on springback. Thipprakmas [8] investigated the effects of punch height on V-die bending process by finite element analysis. He compared the experimental results and finite element results to prove his argument.

Researches related to springback phenomenon in wipe bending process are carried out recently. Nasrollahi and Arezoo [23] investigated springback results of the perforated components in wipe bending. They researched the effects of hole type, number of holes, the ratio of hole width to sheet width, die radius and pad force on springback in wipe bending process. They used FEM results as the training data for ANN and also they compared FEM results with experimental results. Kazan et al. [5] focused on wipe bending process and ANN. They used finite element modeling for wipe bending process and compared the FEA results with ANN results. They focused on effects of sheet thickness, tooling geometry, lubrication conditions, and material properties and processing parameters on springback. Song et al. [24] focused on evaluation of the reliability of different ways of springback angle prediction on the straight flanging operation. They conducted an experiment of straight flanging operation. They discussed prediction approaches such as analytical model, numerical simulation using Finite Element Method (FEM) and Meshfree Method. They compared finite element results with experiment. Ling et al. [25] conducted a parametric study on how the inclusion of a step in the die may reduce springback to reduce time spent on manual corrections of the die. They researched the effects of die clearance, die radius, step height and step distance on springback. Chanthapak et al. [26] investigated influences of bottoming-bead geometry on springback by using finite element method and laboratory experiments are done to validate the FEM simulation. They used low-carbon steel, SPCC (JIS G 3141) and a commercial code.

Air bending is a similar process to V-die bending however differences in die geometry cause varied springback behavior in process. These kinds of differences are researched and springback behavior of air bending is investigated by many researchers. Vin et al. [27] presented “three section” model for air bending. They assumed plain strain condition exists in their study and Bernoulli’s law is valid. They used Swift’s equation to describe material behavior, and addressed change of Young’s modulus under deformation. Their model is capable of generating information such as required punch displacement and the unfolded blank size very accurately. Fu et al. [28] constructed a finite element (FE) model using Hill’s

quadratic anisotropic yield function under the conditions of plane stress and plane strain, respectively. They embedded the improved Hill's yield function into ABAQUS to model single-step air-bending and semiellipse-shaped workpiece multiple-step air-bending tests for WELDOX700, WELDOX900 and OPTIM960 anisotropic sheets. They calculated springback in air bending, thickness strain along the transverse direction and parts profiles. Wang et al. [7] proposed a bending methodology to achieve more accurate final bend angles by controlling punch displacement. They estimated workpiece properties from measured loaded and unloaded bend angles and these estimated properties are used to determine the final punch position required to obtain the desired bend angle after springback. They made a series of experiments and compared the test results with their FE analysis results. Garcia-Romeu et al. [29] studied on springback determination of air bending process. They obtained springback values for different bending angles of aluminum and stainless steel specimens. Fu et al. [6] developed a neural network algorithm for prediction of punch radius problem involving many parameters of air-bending forming. For minimizing the error between the predictive punch radius and the experimental one they used a genetic algorithm (GA) to optimize the weights of neural network. They established 2D and 3D FEM with the predicted punch radius and other geometrical parameters of a tool. They showed that the punch design method is feasible with the prediction model of GA-neural network.

Prediction of springback with the help of artificial neural network (ANN) is a popular and controversial matter these days. Many researches and studies were done related to this topic. Liu et al. [30] proposed a technique based on artificial neural network and genetic algorithm to solve the problem of springback. They used an improved genetic algorithm to optimize the weights of neural network. They achieved more accurate prediction of springback with the GA-ANN model. Ruffini and Cao [31] combined finite element method and neural network model to control the springback including several parameters such as material properties, sheet thickness etc. in an aluminum channel forming process. Inamdar et al. [32] studied effects of network parameters on the mean square error of prediction in ANN. They used experimental data derived from air V-bending process to train the ANN model. They used five input parameters in their ANN model based on back propagation algorithm. Pathak et al. [33] proposed an artificial neural network model to predict the responses of the sheet metal bending process. The proposed neural network model was trained by 44 cases analyzed by using finite element method. Inputs are sheet thickness and die radius; outputs are stresses, strains, springback, loads, etc for the neural network. They tested trained neural network with five new patterns. They concluded that most of neural network results were quite close to the simulation results. Forcellese et al. [34] investigated a neural network control system for the development of an intelligent air bending process. They especially focused on the training set size for predictive performances of the neural networks. They bent aluminum sheets which are in form of different thicknesses to obtain the data base for training. They used their neural network model to predict other bent specimens and they compared the results. Downes et al. [35] developed a technique using an artificial neural network to assist in the design of roll-forming tools. They preferred to study on cold roll-forming since it is highly efficient and economical method for the production of sheet metal products, compared to rival processes but roll-forming has quality problems such as longitudinal curvature. Their technique minimizes the errors of tool design method and superior than trial and error procedure. Cheng et al. [36] used three supervised neural networks to estimate

bending angles formed by a laser. Spot diameter, scan speed, laser power, and workpiece geometries including thickness and length of sheet metal workpiece are the inputs to these neural networks. Regression models of bending angle are used to comparison. To evaluate the performance of these models verification experiments are conducted. It is shown that the radial basis function neural network model is superior to other models in predicting bending angle. Viswanathan et al. [37] controlled springback of a steel channel forming process using an artificial neural network and a stepped binder force trajectory. They used punch trajectory, which reflects variations in material proper ties, thickness and friction condition as the key control parameter in the neural network. They obtained consistent springback angles in experiments using this control scheme.

CHAPTER 3

FINITE ELEMENT MODELING

3.1 Introduction

Finite element modeling and commercially available finite element tools have been used by engineers to model and solve mechanics problems. Nowadays, very complicated, combined and highly nonlinear problems can be modeled with the help of advanced computers. Bending operations are also very complicated and highly nonlinear processes, and can be modeled by employing finite element analysis technique to simulate the operations.

In this study, MSC.MARC/MENTAT was used to model finite element analyses of the bending operations. The software consists of two main programs; namely, MARC and MENTAT. These programs work together to generate geometrical information that defines your structure, analyze your structure and graphically depict the results. MENTAT is responsible of preprocessing and post-processing, while MARC is responsible for analysis. MENTAT prepares and processes data for use with the finite element method. MARC performs linear and nonlinear stress analysis in the static and dynamic regimes [38].

Large deformations occur in bending operations therefore large displacement theory was used to simulate the processes. In solid mechanics, two different approaches are used to describe the kinematics of deformation as Lagrangian description and Eulerian description. All quantities are expressed with respect to the initial configuration in Lagrangian description whereas all quantities are expressed in terms of the current configuration in Eulerian description. Lagrangian Formulation was applied in this study so that finite element mesh was attached to the material and moved through space along with the material. There are also two distinct Lagrangian methods used in solid mechanics problems; Total Lagrangian formulation and Updated Lagrangian formulation.

In the total Lagrangian formulation, all the variables and the equations are expressed with the original undeformed state as the reference whereas in the Updated Lagrangian formulation, all the variables and the equations are expressed with respect to the current configuration acts as the reference state. Updated Lagrangian formulation has been used to simulate bending operations in many simulations [39] . The Updated Lagrangian formulation was also used in this study.

There mainly exist three types of nonlinearity in the finite element analysis. These nonlinearity sources are geometric nonlinearities, material nonlinearities and nonlinear boundary conditions. The main reason of the geometric nonlinearities is that nonlinear relationship between strains and displacements. As the structure deforms the change in geometry is taken into account to form the strain-displacement and hence the equilibrium equations. Large displacement problems are one type of the geometrically nonlinear problems.

The nonlinear relationship between stresses and strains, results in material nonlinearity. Material behavior depends on current deformation state and possibly past history of the deformation. Nonlinear elastic, plastic, viscoelastic, viscoplastic, creep behaviors are some examples for material nonlinearity.

Boundary conditions depend on the deformation of the structure. Impacts, assembly of the mechanical components, sliding frictional interfaces contain nonlinear boundary conditions. These three types of the nonlinearities were present in all applications in this study.

3.2 Finite Element Analysis

All bending operations are appropriate for plane strain assumption in this study and so all case studies were considered as plane strain problems. This assumption simplified the models from 3D to 2D.

Four node, isoparametric, arbitrary quadrilateral elements were used in the analyses. When required the created mesh was converted to a finer mesh by subdividing into smaller elements to overcome the nonlinearities and achieve more accurate results.

In this study, all bending processes were thought as contact problems. In all finite element models, the dies were assumed as rigid and bending occurred with the contact of the bodies in motion. Displacement boundary conditions were employed in wipe bending analyses. Force boundary conditions were not used in this study.

In this study, materials in all case studies were considered as isotropic and elastic-plastic materials. Young's modulus, Poisson's ratio, and representation of the workhardening curve are the input of the program.

In this study, the von Mises yield criterion, also known as maximum distortion energy theory, was used in all finite element analyses.

Coulomb Friction Model was preferred in all of the analyses in this study.

The Coulomb Friction Model is:

$$F_f \leq -\mu F_N \tag{3.1}$$

where

F_f is the friction force exerted by each surface on the other [N]

F_N is the normal reaction force [N]

μ is the coefficient of friction

3.3 The Finite Element Modeling

Air bending, V-die bending, and wipe bending operations are modeled and analyzed using FEM in this study. Input data are the material properties, time vs. velocity tables, boundary conditions, and stress vs. plastic strain tables for modeling. Created finite element models of air bending, V-die bending and wipe bending are shown in Figures 3.1, 3.2, and 3.3.

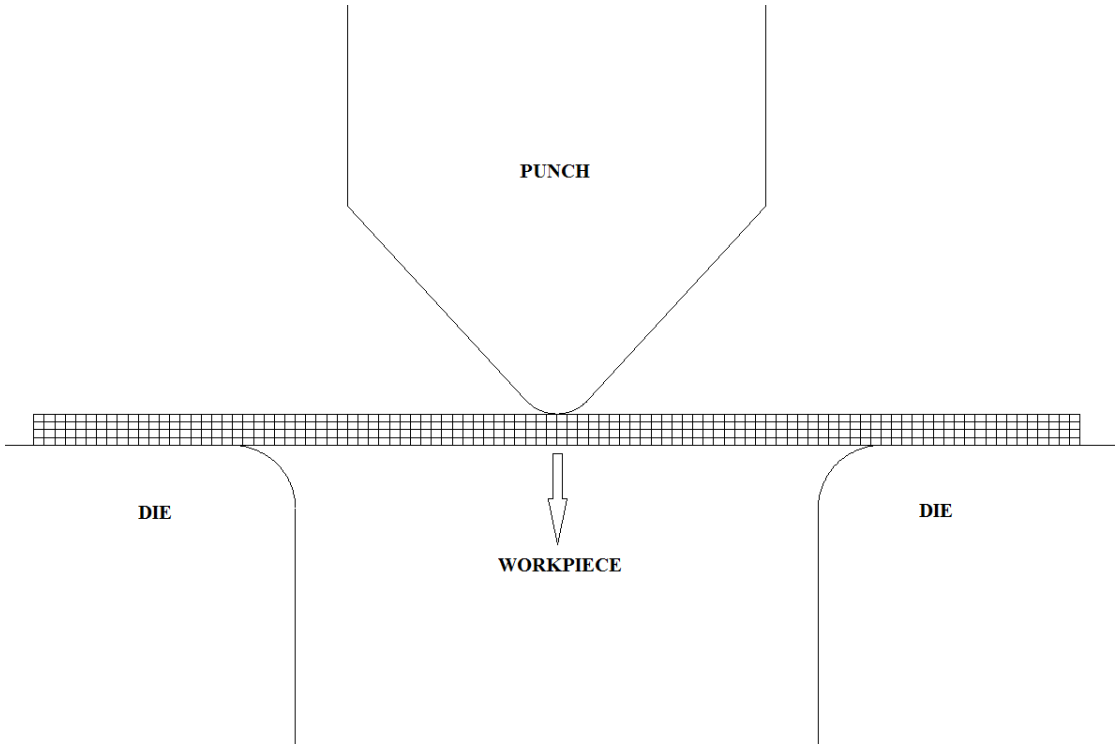

Figure 3.1 FEM of air bending

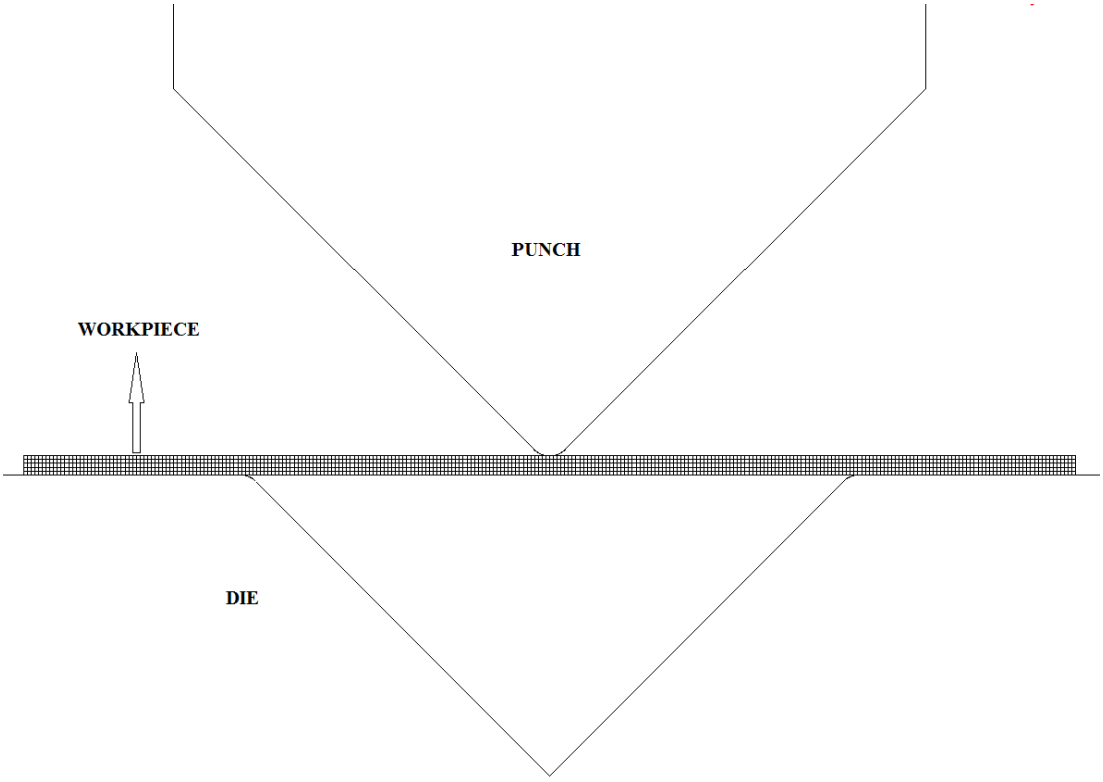

Figure 3.2 FEM of V-die bending

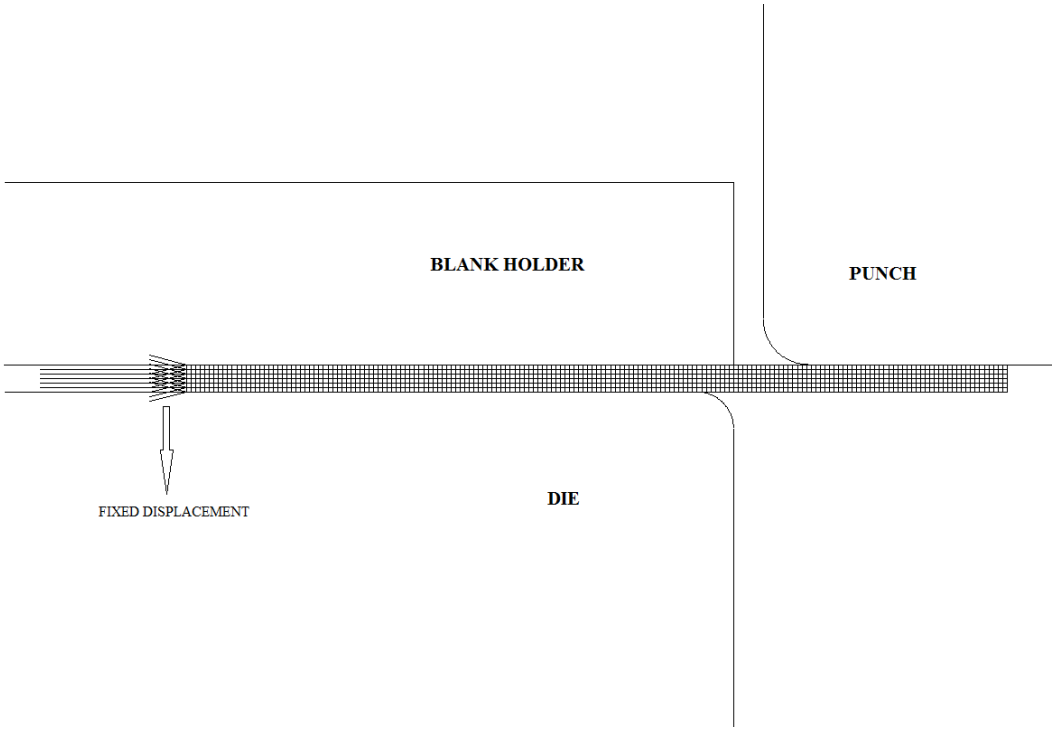

Figure 3.3 FEM of wipe bending

CHAPTER 4

THE ARTIFICIAL NEURAL NETWORK DEVELOPMENT

4.1 Introduction

An artificial neural network (ANN) is a system inspired in the natural neurons that tries to simulate human brain's learning process. Natural neurons receive signals through synapses located on the dendrites or membrane of the neuron. The neuron is activated and emits a signal through the axon when the signals received are strong enough (reach a certain threshold value). This signal might be sent to another synapse, and might activate other neurons [41].

When modeling artificial neurons the complexity of real neurons is imitated. Artificial neural network is an interconnected group of artificial neurons that uses a mathematical model for information processing based on a connectionist approach to computation [42]. Artificial neurons consist of inputs (like synapses), which accepts the input data for training and are multiplied by weights (strength of the respective signals), and then hidden layer receives the data from the input layer and processes the data by a mathematical function which determines the activation of the neuron and finally sends a response to the output layer. In output layer, the outputs of the artificial neuron are computed. In brief, artificial neural networks combine artificial neurons in order to process information. Figure 4.1 shows a neural network model as a simplified model of the human brain. Figure 4.2 also shows the general structure of the artificial neural network system.

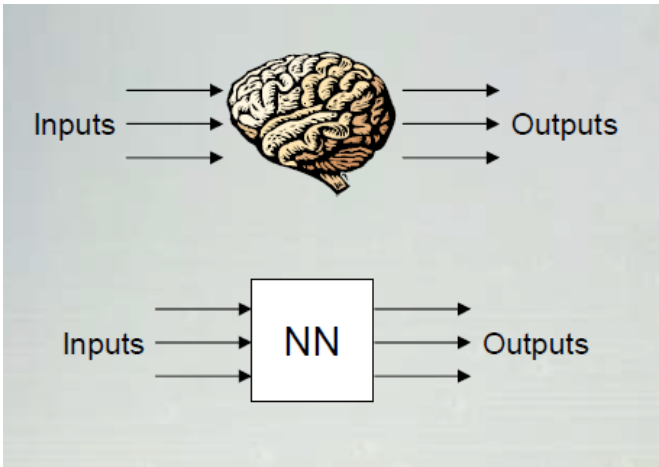

Figure 4.1 Simplified model of the brain [43]

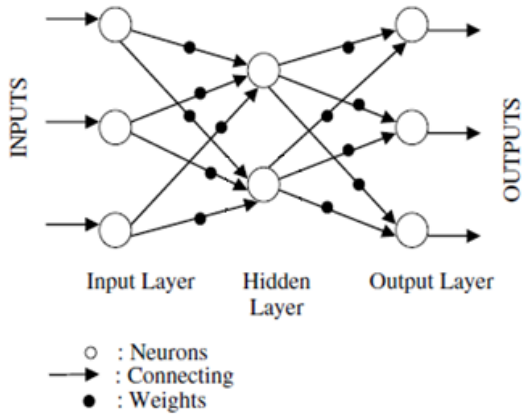

Figure 4.2 The general structure of the artificial neural network system [5]

4.2 Types of the Neural Network according to connection topologies

Neural Network systems can be divided into three main classes, which are single layer neural network, multilayer neural network and recurrent neural network.

4.2.1 Single Layer Neural Network

Single-layer neural network is the simplest kind of neural network, which consists of a single layer of output neurons. The inputs are fed directly to the outputs via a series of weights. In each neuron, the sum of the products of the weights and the inputs are calculated, and if the value exceeds some threshold value (typically 0) the neuron activates and takes the activated value (typically 1); if not it takes the deactivated value (typically -1) [42]. Artificial neurons definition comes from these neurons which have this kind of activation function. Figure 4.3 shows single layer neural network.

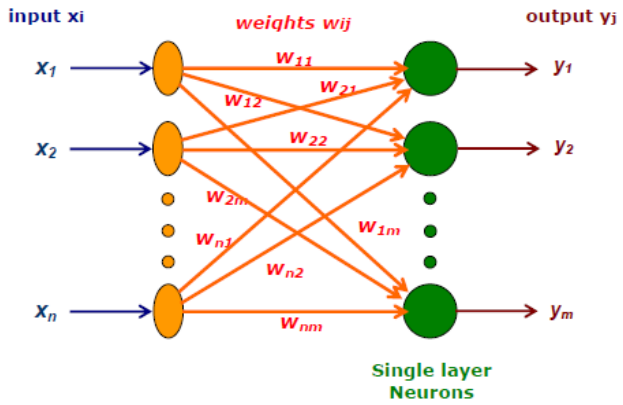

Figure 4.3 Single layer neural network [42]

4.2.2 Multi-Layer Neural Network

Multi-layer neural network consists of multiple layers of computational units, usually interconnected in a feed-forward way. Each neuron has directed connections to the neurons of the subsequent layer in one layer. The architecture of this class of network has one or more intermediary layers called hidden layers. Before directing the input to output layer the hidden layer does intermediate computation. The input layer neurons are linked to hidden layer neurons and hidden layer neurons are linked to output layer neurons. Figure 4.4 illustrates multi-layer neural network. In this study, multi-layer neural network is preferred.

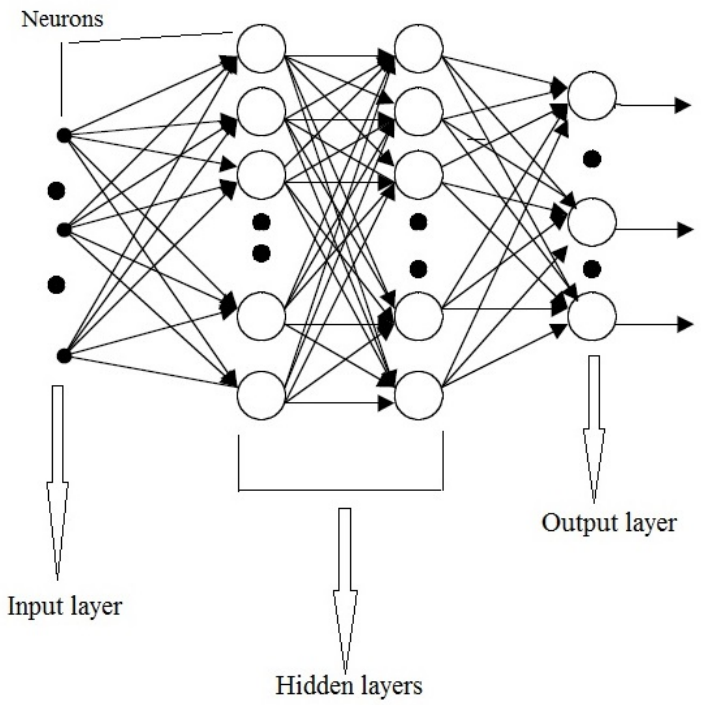

Figure 4.4 Multi-layer neural network [44]

4.2.3 Recurrent Neural Network

A recurrent neural network has at least one feedback loop. There could be neurons with self-feedback links that is the output of a neuron is feedback into itself as input [42]. Recurrent neural network is illustrated in Figure 4.5.

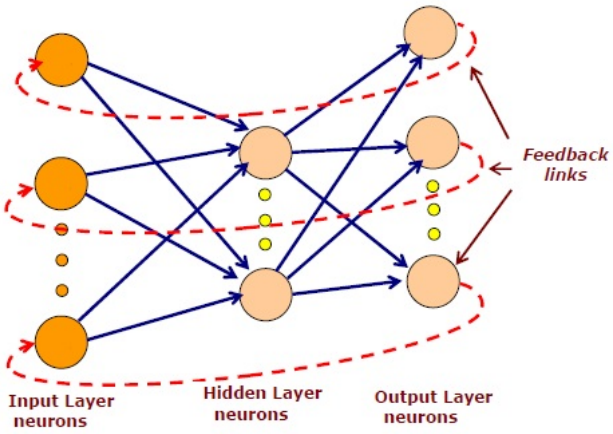

Figure 4.5 Recurrent neural network [42]

4.3 Types of the Neural Network in Terms of Pattern of Connections

Neural Network systems can be divided two main classes according to pattern of connections between the neurons and the propagation of data. These two main classes are feed-forward neural networks and recurrent neural networks.

4.3.1 Feed-forward Neural Networks

The data flow from input to output neurons is strictly transmitted forwards in feed-forward neural networks. The data processing can extend over layers of neurons, but no feedback connections are present, such that, connections extending from outputs of neurons to inputs of neurons are in the same layer or previous layers. Perceptron and Adaline are classical examples of feed-forward neural networks. A feed-forward neural network is used in this study. Feed-forward neural network is illustrated in Figure 4.4.

4.3.2 Recurrent Neural Networks

Recurrent neural networks have feedback connections. The dynamical properties of the network are important contrary to feed-forward networks. The activation values of the neurons undergo a relaxation process in some cases such that the system (neural network structure) will evolve to a stable state in which these activations do not change anymore. In other applications, the change of the activation values of the output neurons is important so that the dynamical behavior constitutes the output of the neural network [45]. Examples of recurrent networks have been presented by Anderson, Kohonen and Hopfield. Recurrent neural network is illustrated in Figure 4.5.

4.4 Learning Algorithms of Neural Networks

Learning (training) means that a neural network accepts the inputs and process them according to its own rules and gives outputs. For the next time it is already taught and gives results as soon as possible. This learning is done by some algorithms. There are three types

of learning algorithms widely-used in neural networks, which are supervised learning (error-based), unsupervised learning and reinforced learning. This classifying is based on presence or absence of a teacher in the system and the information provided for the system to learn.

4.4.1 Supervised (Error-Based) Learning

In this study, supervised learning is chosen, in which the network is trained by providing it with input and matching output patterns. These input-output pairs can be provided by the system which contains the neural network (self-supervised) [45]. In supervised learning, computed output by network and the correct expected output are compared and finally an error is generated. The generated error is used to change network parameters that result in improved performance. In supervised learning a teacher exits during learning (training) process and presents expected output. Figure 4.6 illustrates supervised learning algorithm.

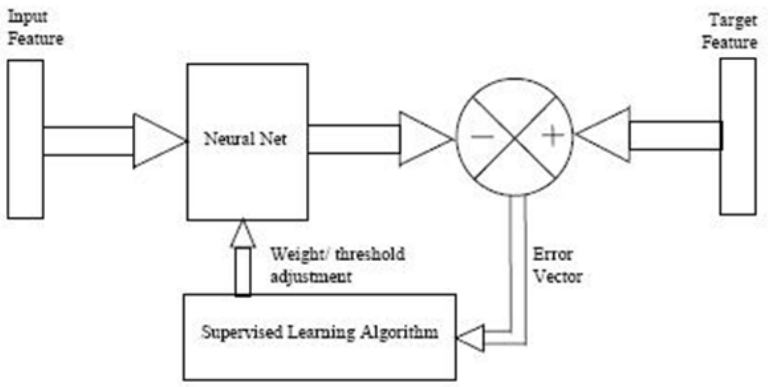

Figure 4.6 Supervised learning algorithm [45]

Supervised learning can be divided in two subclasses namely stochastic and error correction gradient descent.

4.4.1.1 Stochastic Learning

The weights in the system are adjusted in a probabilistic fashion in the stochastic learning. Simulated annealing can be given as an example for this type of learning. Simulated annealing is employed by Boltzmann and Cauchy machines [42].

4.4.1.2 Error Correction Gradient Descent Learning

The essential rule of this learning type is minimization of errors defined in terms of weights. This learning type is based on minimization of errors and the activation function of the network. In this type of learning the activation function must be differentiable because the

updates of weight are dependent on the gradient of the error. Back-propagation algorithm and Least Mean Square algorithm are the examples of Gradient Descent learning [42].

Back-propagation algorithm is a special type of error algorithm and used in multi-layered feed-forward artificial neural networks. In this algorithm, neurons in each layer send their signals forward, and gathered errors are propagated backwards. The inputs are received by input layers and processed in hidden layers and finally the output of the network is given by the neurons on an output layer. Supervised learning is used in the back-propagation algorithm which means that inputs and output are provided to the network to compute and then difference between actual and expected results (error) is calculated. The main idea behind this algorithm is reducing this error until the ANN learns the training data. The procedure says that the training starts with random weights and the system adjust them to achieve minimal error [41].

The activation function of this algorithm used in neurons is a weighted sum:

$$A_j(\overline{x}, \overline{w}) = \sum_{i=0}^{n} x_i w_{ji} \tag{4.1}$$

and the most common output function used in this algorithm is the sigmoidal function:

$$O_j(\overline{x}, \overline{w}) = \frac{1}{1 + e^{A_j(\overline{x}, \overline{w})}} \tag{4.2}$$

The detailed explanation of sigmoidal function is given in the transfer function section. The error of the network can be calculated as summing of the errors of all the neurons in the output layer:

$$E(\overline{x}, \overline{w}, \overline{d}) = \sum_{j} (O_j(\overline{x}, \overline{w}) - d_j)^2 \tag{4.3}$$

From this formula it can be seen that error depends on the output, inputs, and weights. With the help of this formula the weights can be adjusted to minimize the error by the method of gradient descendent:

$$\Delta w_{ji} = -\eta \frac{\partial E}{\partial w_{ji}} \tag{4.4}$$

It is recommended that ANNs implementing the back-propagation algorithm should not have too many layers, because the time for training the networks grows exponentially. In this thesis, back-propagation algorithm is used.
where:

x_i : input

w_{ji} : weight

d_j : output

$\overline{x}$: $\{x_1, x_2, ..., x_n\}$

$\overline{w}$: $\{w_1, w_2, ..., w_n\}$

$\overline{d}$: $\{d_1, d_2, ..., d_n\}$

4.4.2 Unsupervised Learning

In unsupervised learning, training is done such that an output unit is learned to respond to clusters of pattern within the input. In this type of learning network system is supposed to discover statistically salient features of the inputs. Differently from supervised learning, the network learns of desired output owned by discovering and adapting to the structural features in the input patterns [45]. In unsupervised learning a teacher does not exit during learning (training) process and because of that the expected output is not presented to the network. Hebbian Learning and Competitive Learning are two main subclasses of unsupervised learning.

4.4.2.1 Hebbian Learning

Hebbien Learning based on a rule and this rule bases on correlative weight adjustment. The input-output pattern pairs are associated by the weight matrix known as correlation matrix in this rule. Kosko, Anderson and Lippman propose many variations of this rule [42].

4.4.2.2 Competitive Learning

In Competitive Learning, strongly responding neurons to the input actuator have their weights updated. All neurons in the layer compete and the winning neuron undergoes weights adjustment when an input pattern is presented. This phenomenon is called "winner-takes-all" [42].

4.4.3 Reinforced Learning

Reinforced learning can be considered as an intermediate form of the above two types of learning. The training mechanism does some action on the system and gets a feedback response from the system. A teacher exits but does not present the desired output but only grades whether the computed output is correct or incorrect. Generally, parameter adjustment is continued until an equilibrium state occurs, following which there will be no more changes in its parameters [45].

4.5 Transfer (Activation) Functions

The transfer function may be a linear or a nonlinear. To satisfy some specification of the problem that the neuron is attempting to solve a special transfer function is chosen. Most commonly used functions are discussed in this section.

4.5.1 Hard Limit (Threshold) Transfer Function

If the function argument is less than 0, hard limit transfer function sets the output of the neuron to 0, or 1 if its argument is greater than or equal to 0. Function graph is shown in Figure 4.7.

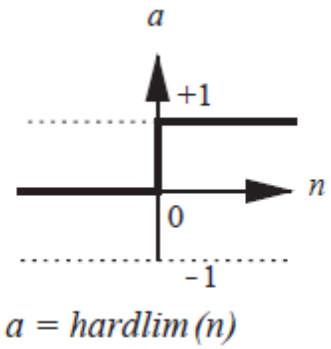

Figure 4.7 Hard limit transfer function [46]

where:

a : neuron output

n : net input

Neuron with hard limit transfer function is called McCulloch-Pitts model [46].

4.5.2 Linear Transfer Function

The output of linear transfer function is equal to its input; $a = n$. It is illustrated in Figure 4.8.

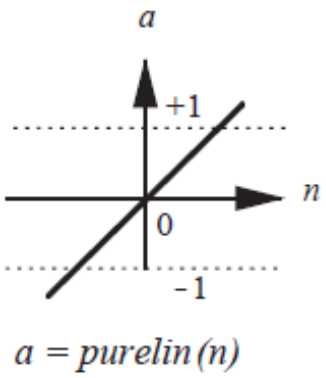

Figure 4.8 Linear transfer function [46]

Neurons with linear transfer function are used in the ADALINE (Adaptive Linear Element) networks.

4.5.3 Log-Sigmoid Transfer Function

Log-sigmoid transfer function takes the input which may change any value between plus and minus infinity and squashes the output into the range 0 to 1, according to the formula [46]:

$$a = \frac{1}{1+e^{-n}} \tag{4.5}$$

This function is a nonlinear curved S-shape function and the most common type of transfer function used in networks. It is commonly used in multilayer networks that are trained using the back-propagation algorithm, in part because this function is mathematically well behaved, differentiable and strictly increasing function as illustrated in Figure 4.9. In this study, the Log-Sigmoid transfer function is used since the network is multilayered and uses back-propagation algorithm.

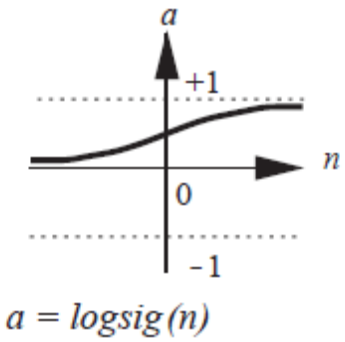

Figure 4.9 Log-sigmoid transfer function [46]

4.6 Training Algorithm

In this study, Levenberg–Marquardt (LM) algorithm is used for training algorithm since the Levenberg-Marquardt algorithm is a robust and rapidly converging method for approximating a function. LM algorithm is a widely used technique for nonlinear least squares problems. LM algorithm is a combination of steepest descent and the Gauss-Newton method. The algorithm behaves like a steepest descent method when the current solution is far from the correct one: slow, but guaranteed to converge. It becomes a Gauss-Newton method when the current solution is close to the correct solution [47]. Levenberg–Marquardt (LM) algorithm consists in solving the equation basically:

$$(J^TJ + \lambda I)\ \delta = J^TE \quad (4.6)$$

Where J is the Jacobian matrix for the network system, λ is the Levenberg's damping factor, I is the identity matrix, δ is the weight update vector that is aimed to be found, and E is the error vector which contains the output errors for each input vector used on training the network. The δ indicates how much network weights should be changed to achieve a (possibly) better solution. The J^TJ matrix is the approximated Hessian. The λ is adjusted at each iteration, and guides the optimization process. A smaller value can be used, bringing the algorithm closer to the Gauss–Newton algorithm if reduction of E is rapid. Whereas if an iteration gives insufficient reduction in the residual, λ can be increased, giving a step closer to the gradient descent direction.

4.7 Performance Function

The mean square error (MSE) function is derived for regression problems. This function can be obtained by the maximum likelihood (ML) principle assuming the independence and Gaussianity of the target data. The created neural network system uses Q sets of input and output data during training. The network adjusts the weights by an iterative algorithm so that the outputs (y_k) according to the input patterns will be as close as possible to their respective desired output patterns (d_k). The mean square error (MSE) function is to be minimized considering a neural network with K which is the total number of outputs as [5]

$$MSE = \frac{1}{QK}\sum_{q=1}^{Q}\sum_{k=1}^{K}[d_k(q) - y_k(q)]^2 \quad (4.7)$$

To minimize MSE by adjusting the weights of connection links, the back-propagation algorithm is most widely used in the network system. The mean square error (MSE) function is also used in this study.

CHAPTER 5

CASE STUDIES AND RESULTS

In this chapter, air bending, V-die bending, and wipe bending operations are modeled and analyzed using FEM. With the help of the analyses, springback amounts are found. Springback results of the bending operations are used in artificial neural network development. FEA results and ANN results are combined to analyze an industrial workpiece used in defense industry at the end of chapter.

The bending operations are considered as plane strain. Four-node quadrilateral plane strain elements are used in the analyses. Coulomb's friction is used to define friction phenomenon between blank holder, sheet, die, and punch. Updated Lagrange procedure is preferred. For the finite element analyses, input data are the material properties, time vs. velocity tables, boundary conditions, stress vs. plastic strain tables, the load cases and the definition of the contact model. In this study, only steel sheets are used.

The developed ANN system is used for springback predictions. Multilayer feedforward backpropagation algorithm is used as the ANN system algorithm. Gathered springback predictions through ANN are compared with FEA results. Then, all FEA and ANN results are combined to investigate the production stages of an industrial workpiece.

5.1 Air Bending

5.1.1 FEA of Air Bending

In this case study, three different bend angles, four different sheet thicknesses, four different types of steels are modeled with different combinations and analyzed to investigate springback amounts and stress distributions. Bending angles are 112°, 116°, and 120°, and sheet thicknesses are 1, 1.5, 2, and 2.5 mm. All steel sheets have modulus of elasticity of 200 GPa and a Poisson’s ratio of 0.3. For elastic – plastic deformation behavior, plastic strain-true stress relations given in Table 5.1 are used. Three of them are obtained from previous research [2, 20]. In these studies, plastic strain-true stress relation for steel 1, steel 2, and steel 3 materials is obtained by tension tests. The data for SS304 material is obtained from simple tension test. The workpieces have the dimensions of 50×50 mm. The necessary dimensions needed to model the processes are illustrated in Figure 5.1.

Table 5.1 Strain hardening data

Steel 1

Plastic Strain	True Stress (MPa)
0	185
0.0243	250
0.0729	330
0.1495	395
0.2195	434
0.2751	445
0.2973	465

Steel 2

Plastic Strain	True Stress (MPa)
0	325
0.0306	375
0.0732	430
0.1224	475
0.1849	511
0.2533	535
0.2740	550

Steel 3

Plastic Strain	True Stress (MPa)
0	286
0.0283	325
0.0690	368
0.1123	405
0.1754	448
0.2278	479
0.2743	503
0.3016	516

Steel 4 (SS304)

Plastic Strain	True Stress (MPa)
0	340
0.0513	410
0.0862	445
0.1040	467
0.1500	510
0.2000	550
0.2950	591
0.3560	610

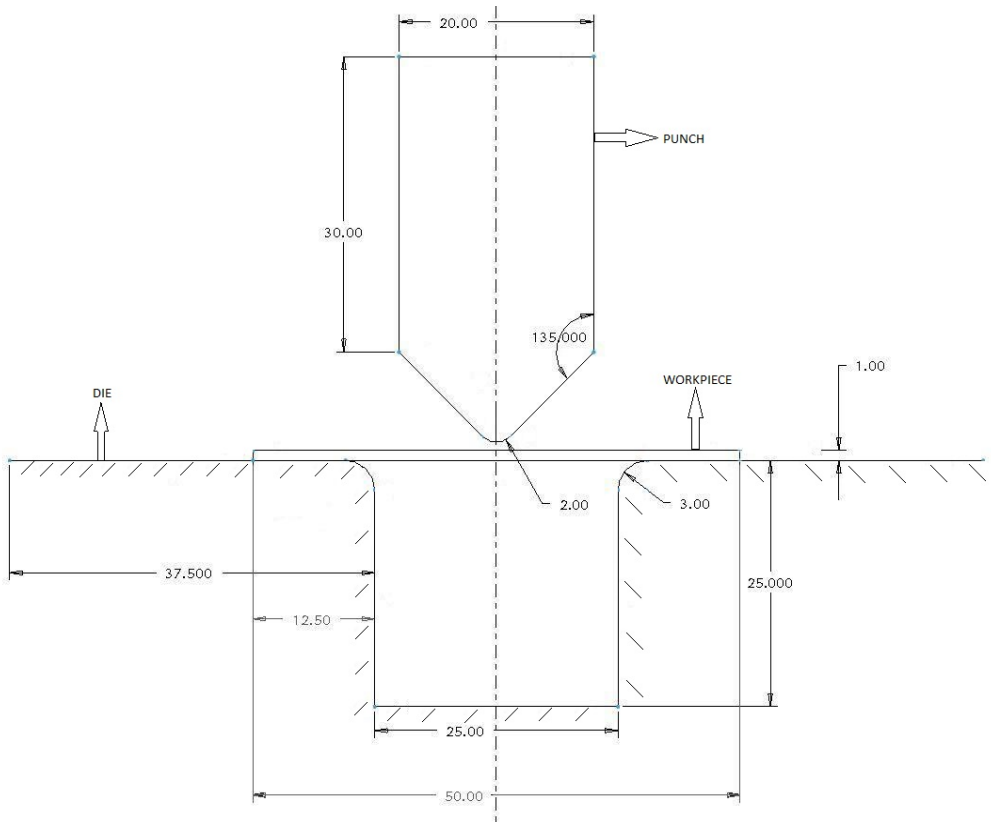

Figure 5.1 Schematic view of air bending with necessary dimensions

As seen from the tables, the yield strength of the steel sheets for steel one, two, three, and four are 185, 325, 286 and 340 MPa respectively. Before the ANN analyses, springback angles (in degrees), equivalent von Misses stress distributions, and stress distributions in the longitudinal direction are presented. Bending and springback angles are illustrated in Figure 5.2. The analyzed models and achieved springback angles are shown in Table 5.2.

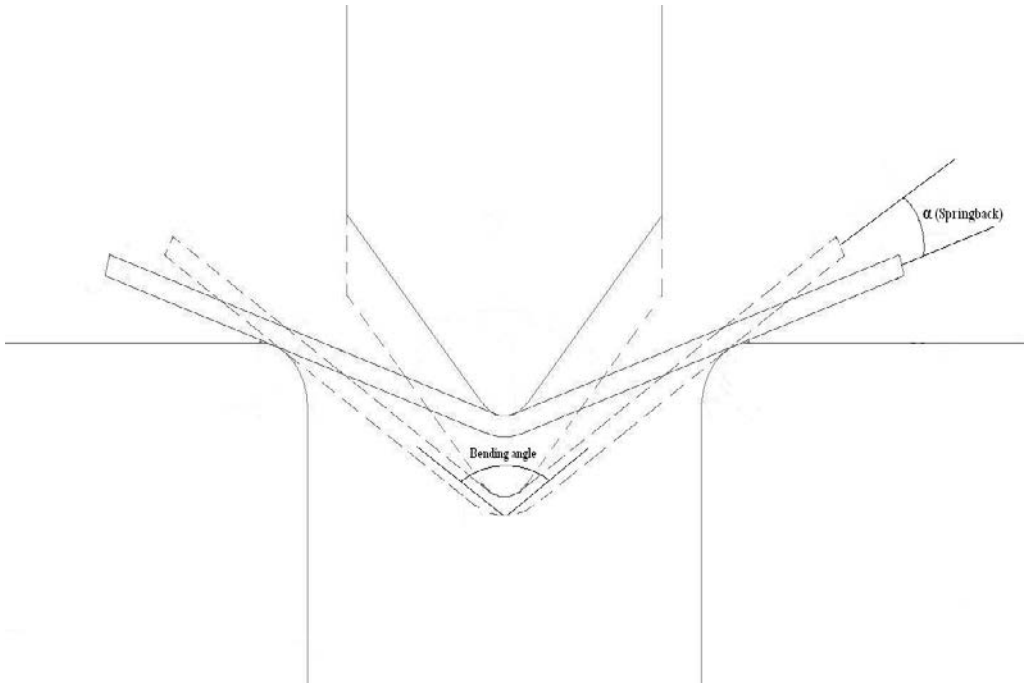

Figure 5.2 Schematic view of air bending angle

Table 5.2 Air bending models and springback results

	Material	**Thickness (mm)**	**Bending angle (°)**	**Springback (°)**
Model 1	Steel 1	1	112	2.37
Model 2	Steel 1	1.5	112	1.73
Model 3	Steel 1	2.5	112	1.17
Model 4	Steel 2	2	116	1.83
Model 5	Steel 2	2.5	116	1.50
Model 6	Steel 3	1	112	2.90
Model 7	Steel 3	1.5	120	2.04
Model 8	Steel 4	1.5	116	2.35
Model 9	Steel 4	2	112	1.90
Model 10	Steel 4	2	116	1.88
Model 11	Steel 4	2	120	1.80
Model 12	Steel 4	2.5	120	1.52

As can be seen from Table 5.2 different combinations of thickness, bending angle, and material are constructed and effects of these parameters on springback are investigated. When model 1 and model 2 are compared it is observed that springback amounts decrease as thickness increases for the same material and same bending angle which is 112°. In a similar manner when model 9 and model 11 are compared it is seen that springback amounts decrease as bending angle increases for the same material and same thickness which is 2 mm. Also when model 1 and model 6 are compared it is found that springback amounts increase as yield strength of the material increases for the same thickness and same bending angle which are 1 mm and 112°, respectively. This result is in agreement with literature [48].

To investigate effects of thickness, bending angle, and yield strength on von Mises stress Table 5.3 constructed.

Table 5.3 Maximum von Mises stress results

	Thickness (mm)	**Bending angle (°)**	**Yield strength (MPa)**	**Max. von Mises stress (fully loaded) (MPa)**	**Max. von Mises residual stress (unloaded) (MPa)**
Model 1	1	112	185	352.8	144.3
Model 2	1.5	112	185	391.3	159.9
Model 6	1	112	286	422.8	208.4
Model 9	2	112	340	564.4	372.3
Model 11	2	120	340	555.5	357.5

When model 1 and model 6 are compared it is observed that material with higher yield strength exhibits much higher maximum von Mises stress values than the material with lower yield strength for the same thickness and same bending angle. When model 1 and model 2 are compared it is found that maximum von Mises stress increases as thickness of the workpiece increases for the same material and same bending angle. When model 9 and model 11 are compared it is seen that maximum von Mises stress decreases slightly as bending angle increases for the same material and same thickness. Variations of thickness and bending angle are effective on maximum von Mises stress distributions but the dominant factor is observed to be the yield strength of the materials. Also, there occurs an important drop in the value of the maximum von Mises stress values after the backing of the punch for all operations.

In addition to the aforementioned observations, other types of stress distributions are also investigated. In Figures 5.3 and 5.4, von Mises stress distribution in steel 3 for 1-mm-thick sheet with 112° bending angle are illustrated.

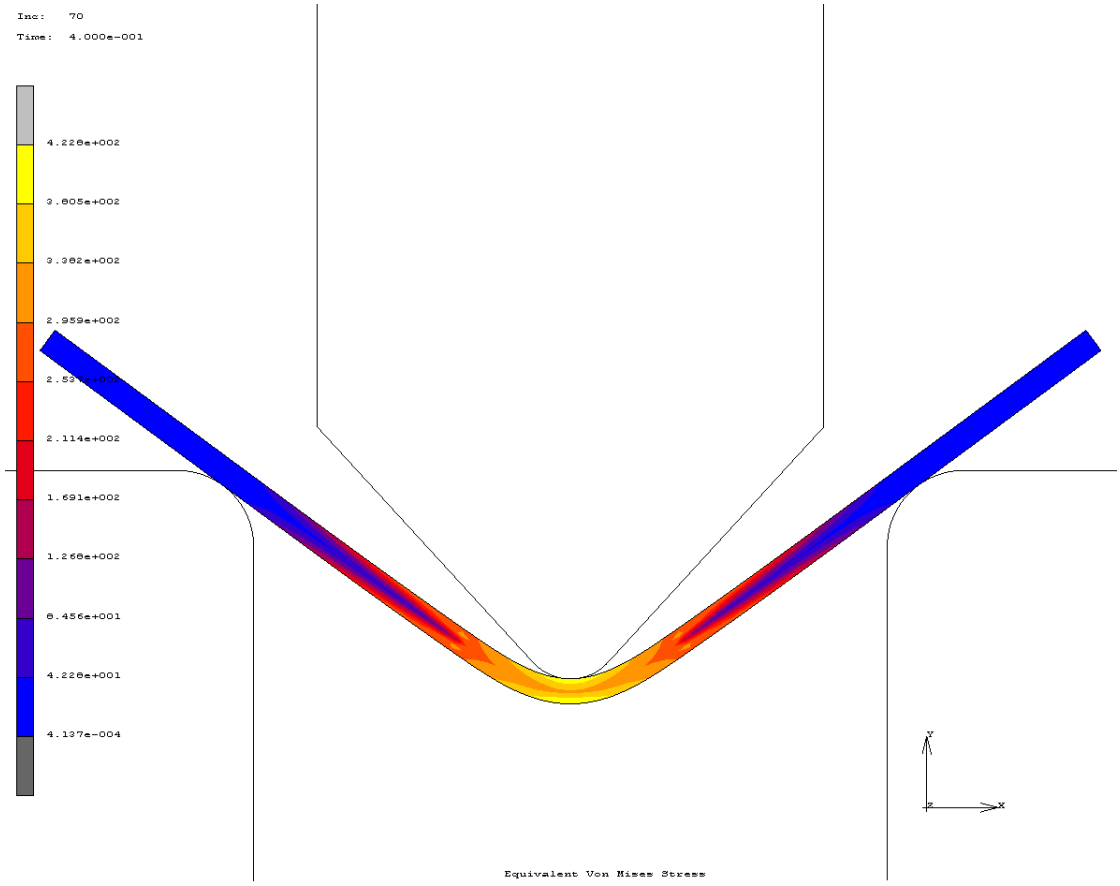

Figure 5.3 Von Mises stress distribution in steel 3 for 1-mm-thick sheet with 112° bending angle at fully loaded stage

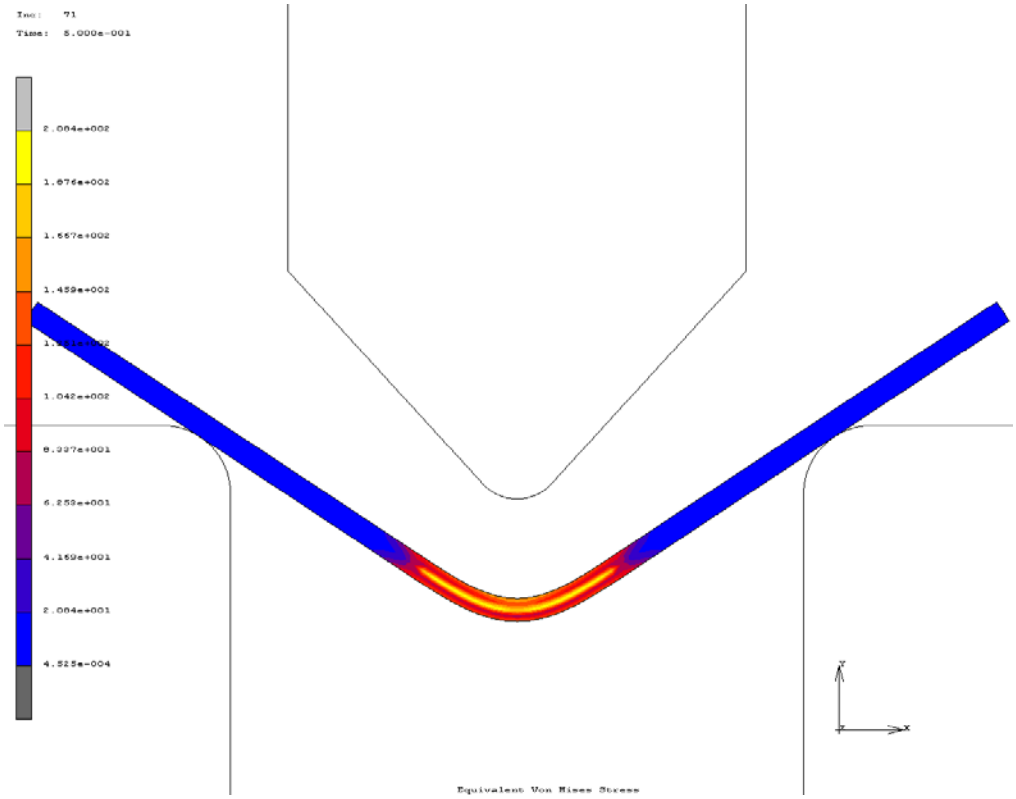

Figure 5.4 Residual von Mises stress distribution in steel 3 for 1-mm-thick sheet with 112° bending angle at unloaded stage

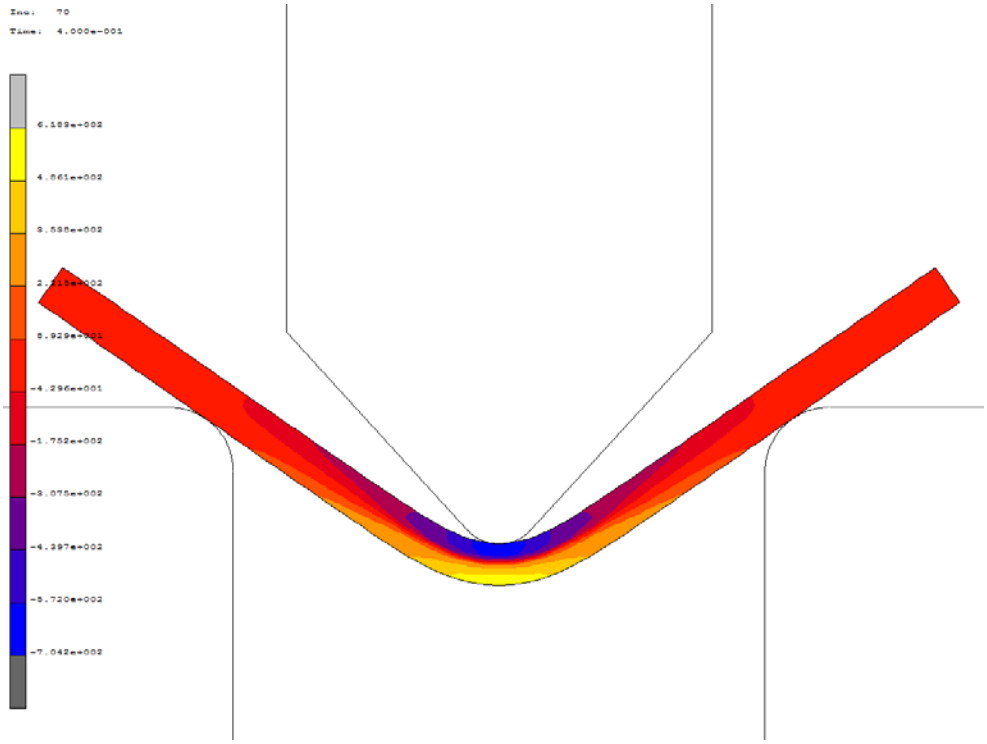

Figure 5.5 Normal stress distribution in longitudinal direction in steel 4 for 2-mm-thick sheet with 116° bending angle at the fully loaded stage

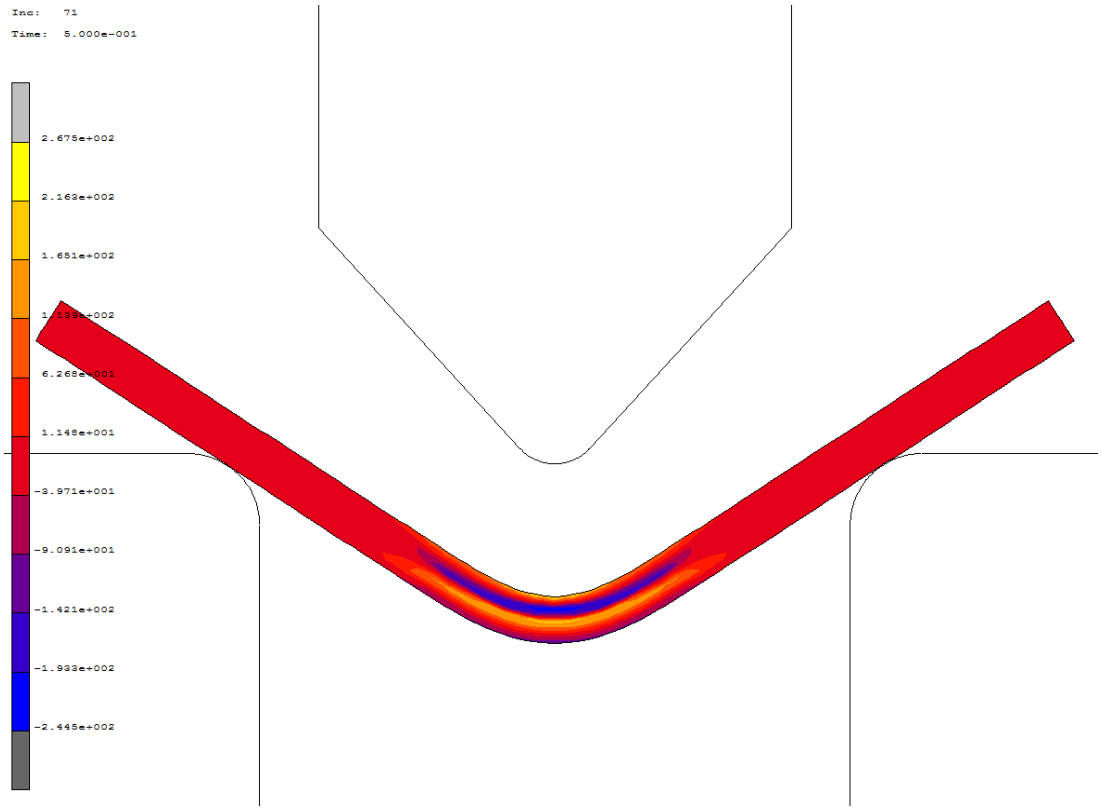

Figure 5.6 Residual normal stress distribution in longitudinal direction in steel 4 for 2-mm-thick sheet with 116° bending angle at the unloaded stage

In Figures 5.5 and 5.6, normal stresses in longitudinal direction in steel 4 (SS304) for 2-mm-thick sheet with 116° bending angle are illustrated.

Figures 5.5 and 5.6 show that at the fully loaded stage, the midst of the sheet about the neutral axis is in elastic regime, while the outer (inner and outer) fibers are in plastic regime. After unloading, residual stresses appear and the distribution of the residual stresses is in agreement with theoretical information. Inner fibers of the workpiece are under compression while outer fibers of the workpiece are in tension. Figures 5.3 and 5.4 also verify the expected von Mises stress distribution, which is localized in the bent-up region in bending process.

5.1.2 ANN Development of Air Bending

In order to predict springback amounts without using FEA and investigate the suitability of artificial neural networks in bending operations, an artificial neural network structure is developed. Table 5.4 illustrates the general structure of the developed ANN system.

Table 5.4 General structure of the developed ANN system

Neural Network Structure	
Network type	Multi-layer
Pattern of connections	Feed-forward
Learning algorithm	Supervised (backpropagation)
Transfer function	Log-Sigmoid function
Training function	Levenberg-Marquardt
Performance function	Mean squared error

To see the effects of the different material usage in terms of strain hardening behavior on springback in ANN, discrete plastic strain-true stress data are converted to Ludwig-Hollomon's equation [49] by regression:

$$\sigma = K\varepsilon_p^{\,n} \tag{5.1}$$

where

σ : true stress
K : strength coefficient (MPa)
ε_p : plastic true strain
n : strain hardening exponent

Calculated *K* and *n* values for steels by regression method is shown in Table 5.5

Table 5.5 Calculated K and n values

	***K*(MPa)**	***n***
Steel 1	635	0.25
Steel 2	683	0.17
Steel 3	721	0.33
Steel 4	754	0.21

ANN system basically consists of two main data sets; namely, training data and testing data. Firstly, ANN system learns the general structure of the information given to it in training part and then within the testing part, validation is carried out. For air bending part, training data set, which is collected from FEA, is given in Table 5.6. For training, ten models are used. Models 5 and 10 are used for the testing part. Testing data set is given in Table 5.7.

Table 5.6 Training data set

	Thickness (mm)	**Bending angle (°)**	**K (MPa)**	**n**	**Springback (°)**
Model 1	1	112	635	0.25	2.37
Model 2	1.5	112	635	0.25	1.73
Model 3	2.5	112	635	0.25	1.17
Model 4	2	116	683	0.17	1.83
Model 6	1	112	721	0.33	2.90
Model 7	1.5	120	721	0.33	2.04
Model 8	1.5	116	754	0.21	2.35
Model 9	2	112	754	0.21	1.90
Model 11	2	120	754	0.21	1.80
Model 12	2.5	120	754	0.21	1.52

Table 5.7 Testing data set

	Thickness (mm)	**Bending angle (°)**	**K (MPa)**	**n**	**Springback (°)**
Model 5	2.5	116	683	0.17	1.50
Model 10	2	116	754	0.21	1.88

Main aim of the ANN system is to predict necessary design and manufacturing parameters for a selected bending operation while minimizing or eliminating the need of possibly time consuming, FEA analyses. As the next step, different bending ANN systems, such as for air bending, wipe bending, etc., can be combined to calculate springback amount for complicated operations and products quickly. In this developed ANN system, springback prediction depends on four independent parameters which are thickness, bending angle, strength coefficient, and straining hardening exponent. Each parameter affects springback independently. ANN system combines these four different aspects and tries to draw a general pattern to achieve the final sprinback amount.

Training and testing parts are carried out within MATLAB software. ANN system's training part is started with 3 hidden layers for air bending as an initial guess. Results are compared with testing data and doing so, different number of hidden layers and percentages are tested to achieve close results. In this section, eight and ten hidden layer numbers are investigated to show the robustness of the ANN algorithm. Finally for eight and ten number of hidden layers, close results are achieved and tested. These results are given in Table 5.8.

Table 5.8 ANN Testing Results

8 Hidden Layers					
	Thickness (mm)	**Bending angle (°)**	**K (Mpa)**	**n**	**Springback (°)**
Model 5	2.5	116	683	0.17	1.48
Model 10	2	116	754	0.21	1.85

10 Hidden Layers					
	Thickness (mm)	**Bending angle (°)**	**K (MPa)**	**n**	**Springback (°)**
Model 5	2.5	116	683	0.17	1.55
Model 10	2	116	754	0.21	1.90

After testing results are achieved, they are compared with testing data, which are FEA results, and relative errors in percentage are given in Table 5.9.

Table 5.9 Relative errors in percentage

					Springback (°)		
	Thickness (mm)	**Bending angle (°)**	**K (MPa)**	**n**	**FEA**	**8 Hidden Layers**	**Error (%)**
Model 5	2.5	116	683	0.17	1.50	1.48	1.33
Model 10	2	116	754	0.21	1.88	1.85	1.60

					Springback (°)		
	Thickness (mm)	**Bending angle (°)**	**K (Mpa)**	**n**	**FEA**	**10 Hidden Layers**	**Error (%)**
Model 5	2.5	116	683	0.17	1.50	1.55	3.33
Model 10	2	116	754	0.21	1.88	1.90	1.06

Table 5.9 clearly shows that the constructed ANN systems with the selected parameters are highly capable of predicting springback. ANN system with 8 hidden layers gives results with relative errors less than 1.60 percent. ANN system with 10 hidden layers is capable of achieving results with relative errors less than 3.33 percent. 8 hidden layers seems to more appropriate for model 5 while 10 hidden layers seems to more appropriate for model 10. The

reason of that is ANN system seeks dual solution for model 5 and model 10 at the same time and relative error of one of them decreases while the other one's increases. This approach is the nature of the ANN algorithm. Table 5.9 emphasizes that developed ANN systems are feasible and robust. Both ANN systems give very close results for two different air bending models' springback predictions.

5.2 V-die Bending

5.2.1 FEA of V-die Bending

In this case study, two different bending angles, three different sheet thicknesses, four different types of steels, and three different punch radii are modeled as different combinations and analyzed to investigate springback amounts and stress distributions. Bending angles are 85°, and 90°. Sheet thicknesses are 1.5, 2, and 2.5 mm and punch radii are 2, 3, and 4 mm. The workpieces have the dimensions of 140×50 mm. The dimensions of the punch, die, and sheet are illustrated in Figure 5.7.

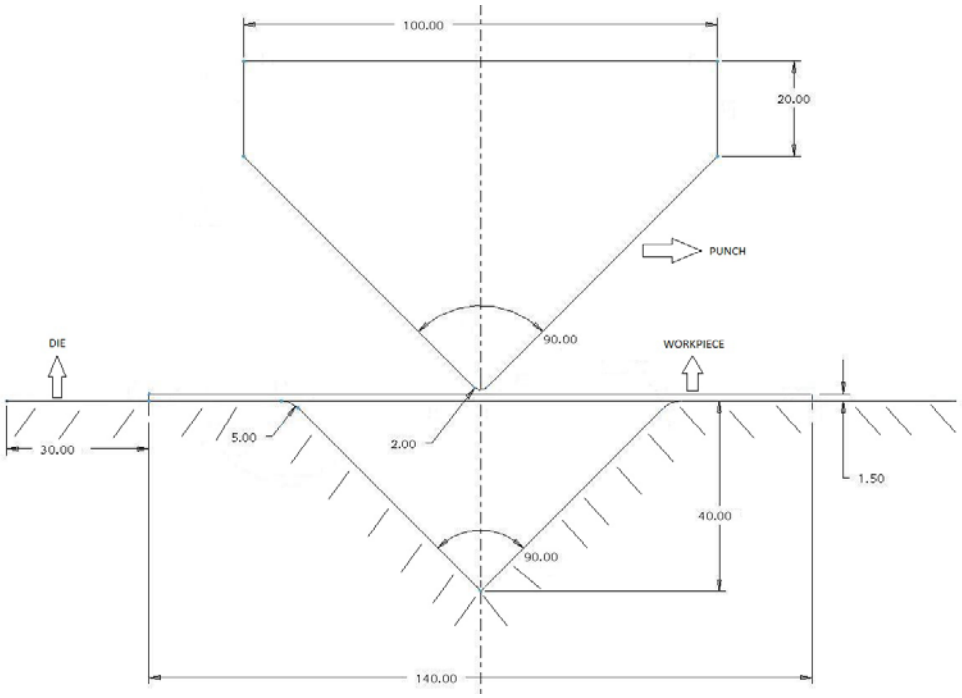

Figure 5.7 Schematic view of V-die bending with necessary dimensions

Bending angle is illustrated in Figure 5.8. The created bending models and achieved springback angles are shown in Table 5.10.

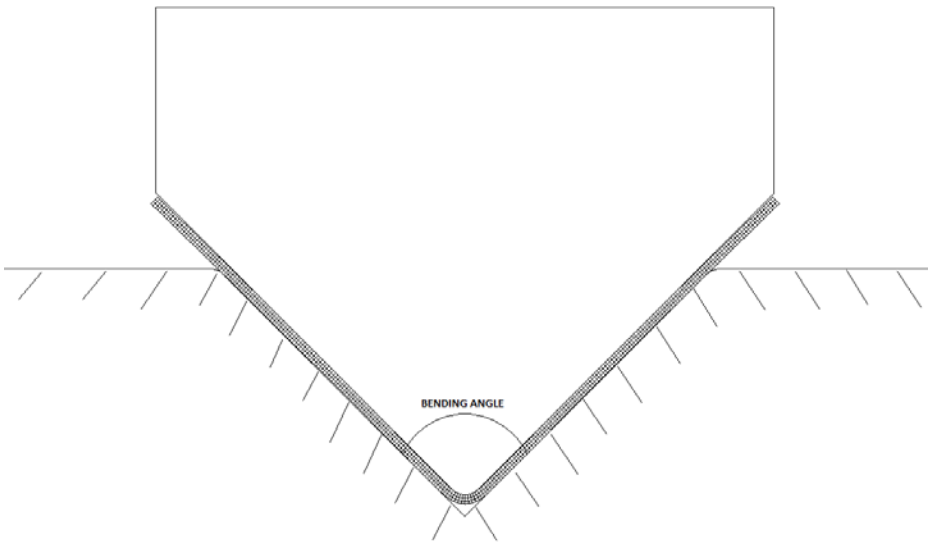

Figure 5.8 Schematic view of V-die bending angle

Table 5.10 V-die bending models and springback results

	Material	Thickness (mm)	Punch radius (mm)	Bending angle (°)	Springback (°)
Model 1	Steel 1	1.5	2	85	-1.21
Model 2	Steel 1	1.5	3	90	-1.47
Model 3	Steel 1	2.5	3	85	-0.70
Model 4	Steel 2	1.5	4	85	-1.80
Model 5	Steel 2	2	2	85	-1.87
Model 6	Steel 2	2	4	90	-1.55
Model 7	Steel 3	1.5	4	90	-1.72
Model 8	Steel 3	2	3	85	-1.58
Model 9	Steel 3	2.5	2	90	-1.36
Model 10	Steel 4	1.5	4	85	-2.01
Model 11	Steel 4	2	2	90	-1.91
Model 12	Steel 4	2.5	3	90	-1.30

Table 5.10 shows that different combinations of punch radius, thickness, bending angle, and material properties.

Secondary bent-up regions cause springback in the opposite direction to the one resulted by the main bent-up region (springforward). In Table 5.10, springback angles are negative as workpiece's arms do not collectively move outwards; however on the contrary tend to move inwards. This phenomenon shows that springback amounts in secondary bent-up regions are

greater than springback amounts in main bent-up region as depicted in Figure 5.9 Primary and secondary bent-up regions in V-die bending.

From Table 5.10, it is observed that springback amounts decrease as punch radius increases. Also, springback amounts decrease as thickness of workpiece and bending angle increases. It is also seen that springback amounts increase as yield strength of the material increases.

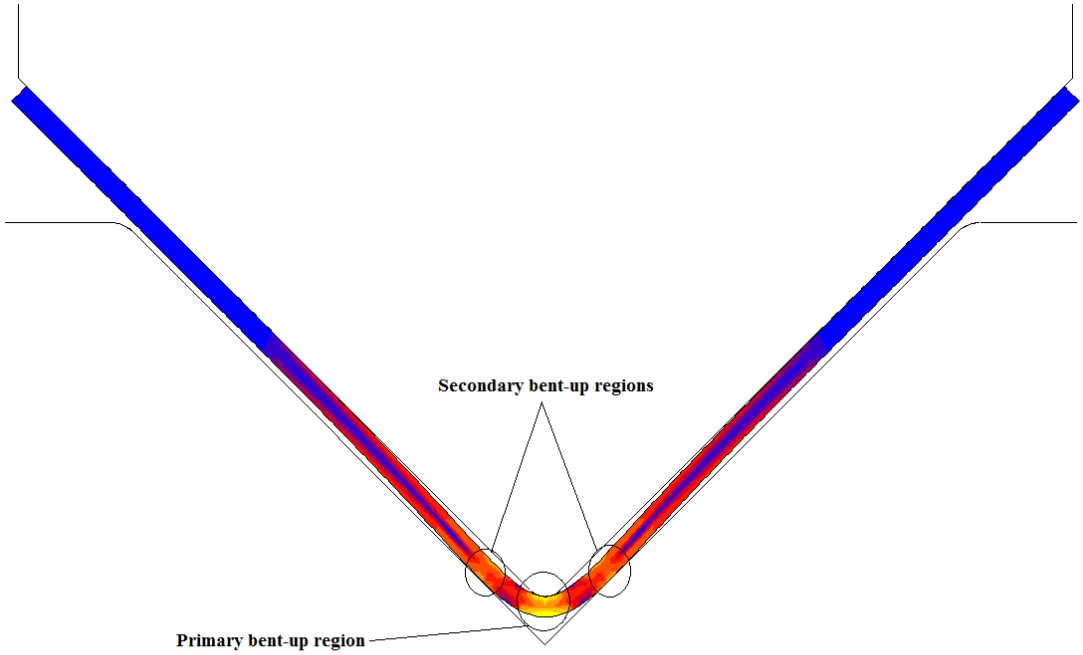

Figure 5.9 Primary and secondary bent-up regions in V-die bending

Table 5.11 shows the effects of punch radius, thickness, bending angle, and yield strength on von Mises stress.

Table 5.11 Maximum von Mises stress results

	Thickness (mm)	Punch radius (mm)	Bending angle (°)	Yield strength (MPa)	Max. von Mises stress (fully loaded) (MPa)	Max. von Mises residual stress (unloaded) (MPa)
Model 2	1.5	3	90	185	475.5	257.6
Model 3	2.5	3	85	185	514.2	438.3
Model 6	2	4	90	325	540.1	318.4
Model 11	2	2	90	340	623.5	531.9
Model 12	2.5	3	90	340	597.4	421.4
Model 13	2	2	93.5	340	612.2	441.6

When model 11 and model 13 are compared it is observed that material which is exposed to larger bending angle exhibits slightly lower maximum von Mises stress values than the material which is exposed to lower bending angle for the same material, same thickness, and same punch radius. When model 6 and model 11 are compared it is found that maximum von Mises stress decreases as punch radius increases for the same thickness, same bending angle and nearly the same yield strength. When model 2 and model 3 are compared it is seen that maximum von Mises stress decreases slightly as thickness of the workpiece decreases for the same material and same punch radius. In this case bending angle is also effective but it does not seem to prevent from the effect of thickness. When model 3 and model 12 are compared it is observed that material with higher yield strength exhibits much higher maximum von Mises stress values than the material with lower yield strength for the same punch radius and same thickness. Also, there is an important drop in the value of the maximum von Mises stress values after the backing of the punch for all operations.

In addition to the aforementioned observations, other types of stress distributions are also investigated. In Figures 5.10 and 5.11, von Mises stress distributions in steel 4 (SS304) for 2.5-mm-thick sheet with 90° bending angle and 3 mm punch radius are illustrated.

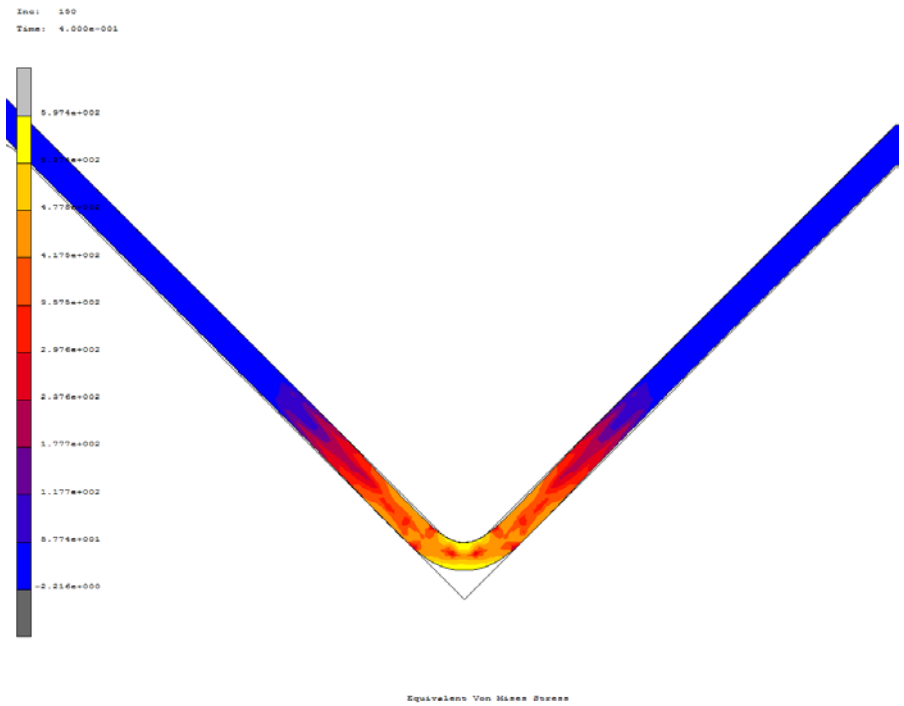

Figure 5.10 Von Mises stress distribution in steel 4 (SS304) for 2.5-mm-thick sheet with 90° bending angle and 3 mm punch radius at fully loaded stage

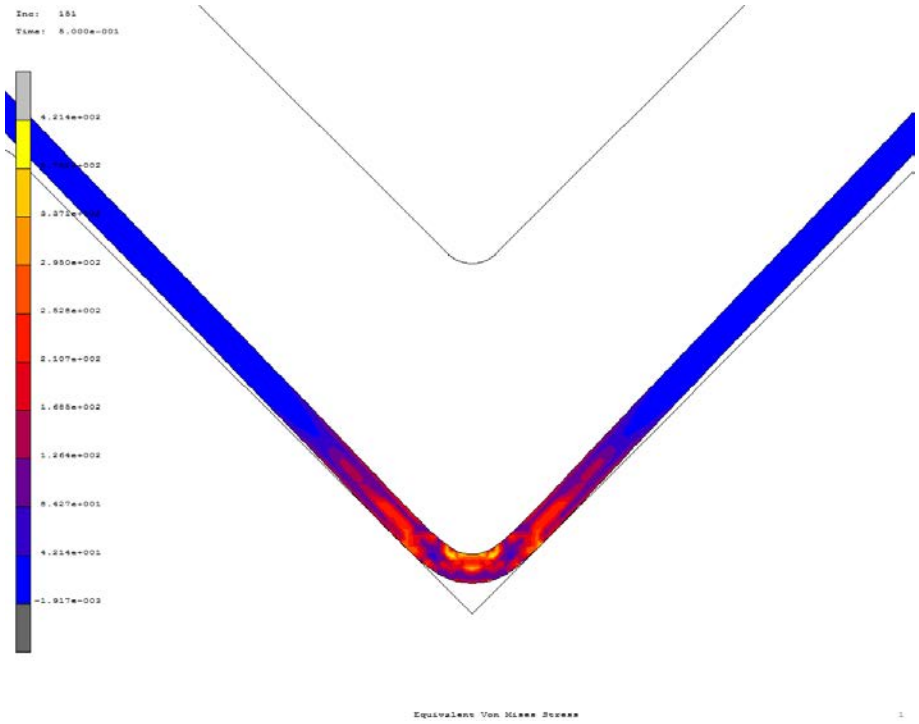

Figure 5.11 Resiual von Mises stress distribution in steel 4 (SS304) for 2.5-mm-thick sheet with 90° bending angle and 3 mm punch radius at unloaded stage

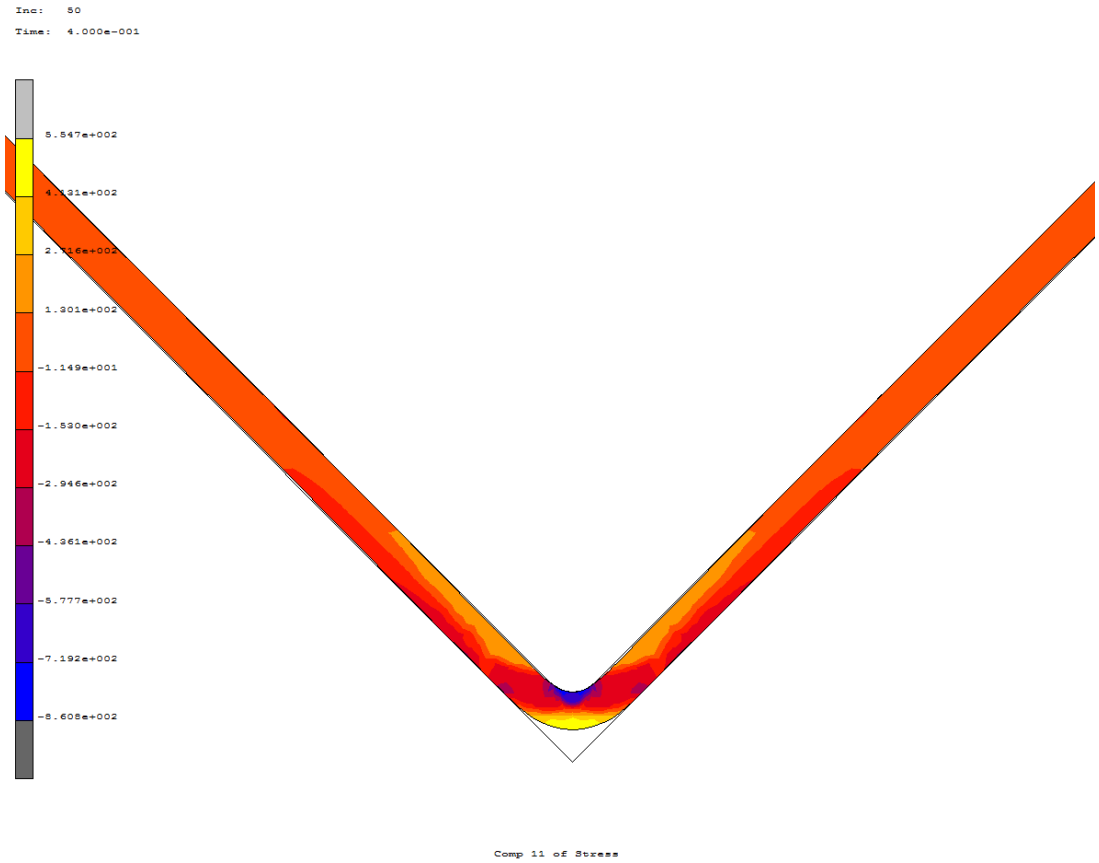

Figure 5.12 Normal stress distribution in longitudinal direction in steel 3 for 2.5-mm-thick sheet with 90° bending angle and 2 mm punch radius at the fully loaded stage

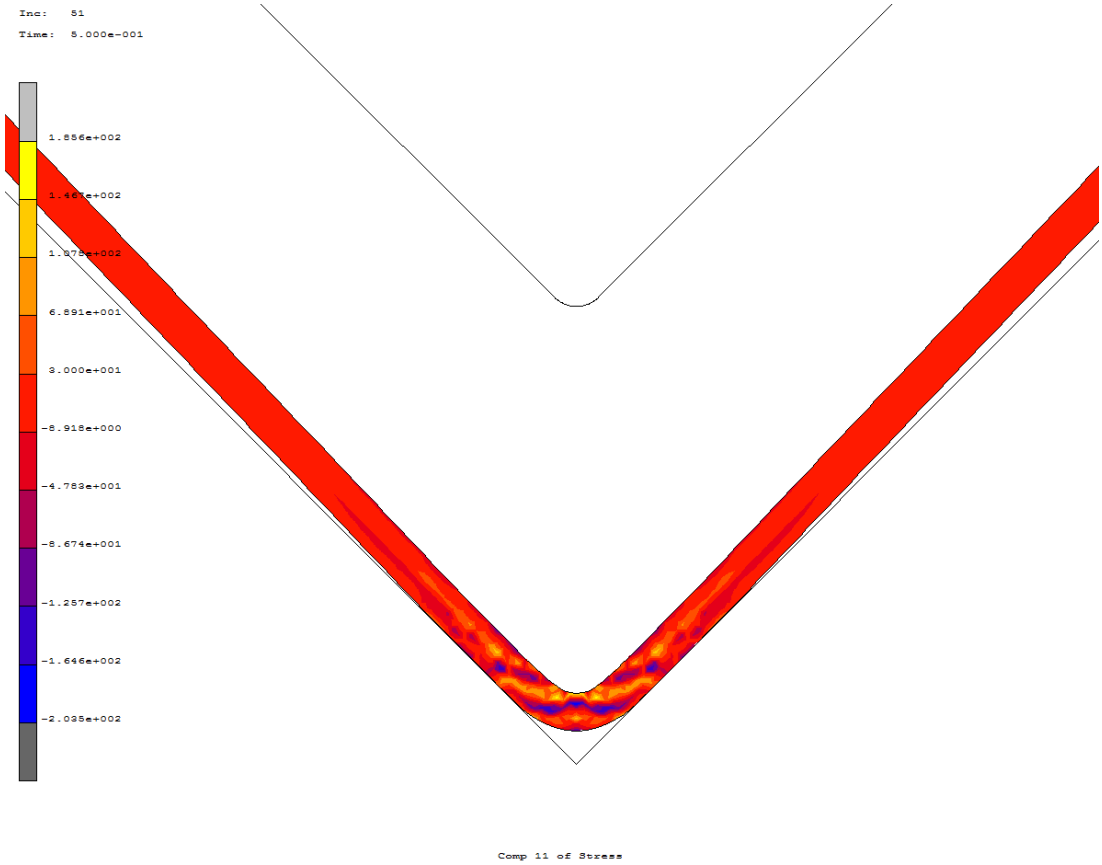

Figure 5.13 Residual normal stress distribution in longitudinal direction in steel 3 for 2.5-mm-thick sheet with 90° bending angle and 2 mm punch radius at unloaded stage

In Figures 5.12 and 5.13, normal stresses in longitudinal direction in steel 3 for 2.5-mm-thick sheet with 90° bending angle and 2 mm punch radius are illustrated.

From Figures 5.12 and 5.13, it is observed that normal stresses along the longitudinal direction at the fully loaded stage, and the residual stress distribution in the unloaded stage appeared. From Figures 5.10 and 5.11, it is seen that higher stress values shown with lighter color are obtained in the bent-up region.

5.2.2 ANN Development of V-die Bending

To predict springback amounts without using FEA for V-die bending operations, the developed artificial neural network structure is utilized. Training data set for V-die bending ANN system is given in Table 5.12. For training, twelve models are used. For testing part, a new model with a new bending angle, which is 93.5°, is constructed and springback result from FEA is achieved. This new model is named as Model 13.Testing data is given in Table 5.13.

Table 5.12 Training data set

	Thickness (mm)	Punch radius (mm)	Bending angle (°)	K (MPa)	n	Springback (°)
Model 1	1.5	2	85	635	0.25	-1.21
Model 2	1.5	3	90	635	0.25	-1.47
Model 3	2.5	3	85	635	0.25	-0.70
Model 4	1.5	4	85	683	0.17	-1.80
Model 5	2	2	85	683	0.17	-1.87
Model 6	2	4	90	683	0.17	-1.55
Model 7	1.5	4	90	721	0.33	-1.72
Model 8	2	3	85	721	0.33	-1.58
Model 9	2.5	2	90	721	0.33	-1.36
Model 10	1.5	4	85	754	0.21	-2.01
Model 11	2	2	90	754	0.21	-1.91
Model 12	2.5	3	90	754	0.21	-1.30

Table 5.13 Testing data set

	Thickness (mm)	Punch radius (mm)	Bending angle (°)	K (MPa)	n	Springback (°)
Model 13	2	2	93.5	754	0.21	-1.82

In the constructed ANN system, springback depends on five independent parameters as punch radius, thickness, bending angle, strength coefficient, and straining hardening exponent. ANN system combines these five different parameters and attempts to draw a general pattern to achieve the final springback amount. To see the effects of the training set size on hidden layer number and accuracy of result, twelve input models are used in training data sets and only one testing data is used.

Training part is started with two hidden layers. Different hidden layer numbers, different training and testing percentages are tried and close results are achieved with only five hidden layers. Result is computed as -1.83° as seen in Table 5.14

Table 5.14 ANN Testing Result

5 Hidden Layers						
	Thickness (mm)	**Punch radius (mm)**	**Bending angle (°)**	**K (MPa)**	**n**	**Springback (°)**
Model 13	2	2	93.5	754	0.21	-1.83

Gathered ANN result is compared with the testing data which is FEA result and relative percentage error is calculated as given in Table 5.15.

Table 5.15 Relative error in percentage

						Springback (°)		
	Thickness (mm)	**Punch radius (mm)**	**Bending angle (°)**	**K (MPa)**	**n**	**FEA**	**5 Hidden Layers**	**Error (%)**
Model 13	2	2	93.5	754	0.21	-1.82	-1.83	0.55

From Table 5.15, it is seen that ANN system for model 13 with five hidden layers gives almost the same result with the FEA result. The percentage error is 0.55. It is observed that if number of training input increases, ANN system requires less hidden layers and converges immediately. Accuracy of the ANN system's result increases with increasing training input/testing input ratio. Training input/testing input ratio is 12/1 in this system. Table 5.15 also shows that ANN systems can be used for extrapolation. In the training data set there is no input with 93.5° bending angle but ANN system predicted result with 0.55 percentage error. This result verifies reliability of the developed ANN system for V-die bending.

5.3 Wipe Bending

5.3.1 FEA of Wipe Bending

Three different sheet thicknesses, three different punch radii, and four different types of steels are modeled with different combinations and analyzed to investigate springback amounts and stress distributions. Bending angle is fixed to 90°. Sheet thicknesses are 1.5, 2, and 3 mm and die radii are 2, 4, and 6 mm. All steel sheets are same as in air and V-die bending sections and have Poisson's ratio of 0.3 and elastic modulus of 200 GPa. The workpieces have the dimensions of 100 × 50 mm. The necessary dimensions to model the processes are illustrated in Figure 5.14. In the models, clearance is taken constant as 0.25 mm.

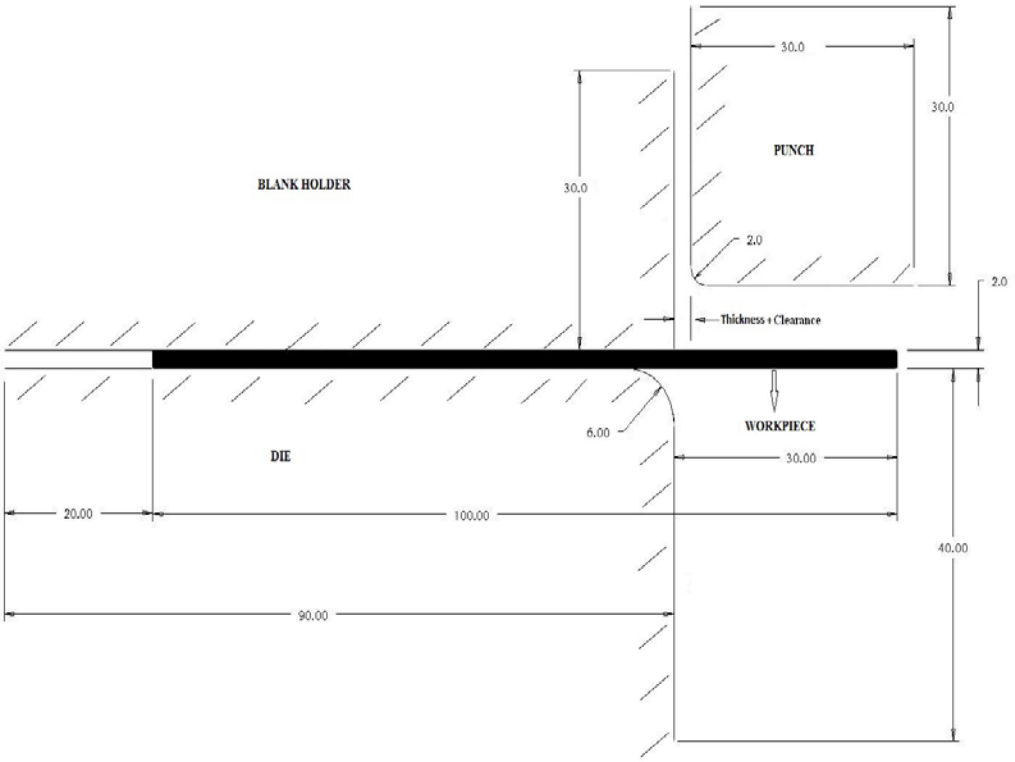

Figure 5.14 Schematic view of wipe bending with necessary dimensions

Springback angles (in degrees), and stress distributions are computed via FEA before starting the ANN analyses. Representative springback angle is illustrated in Figure 5.15. The created bending models and achieved springback angles are shown in Table 5.16.

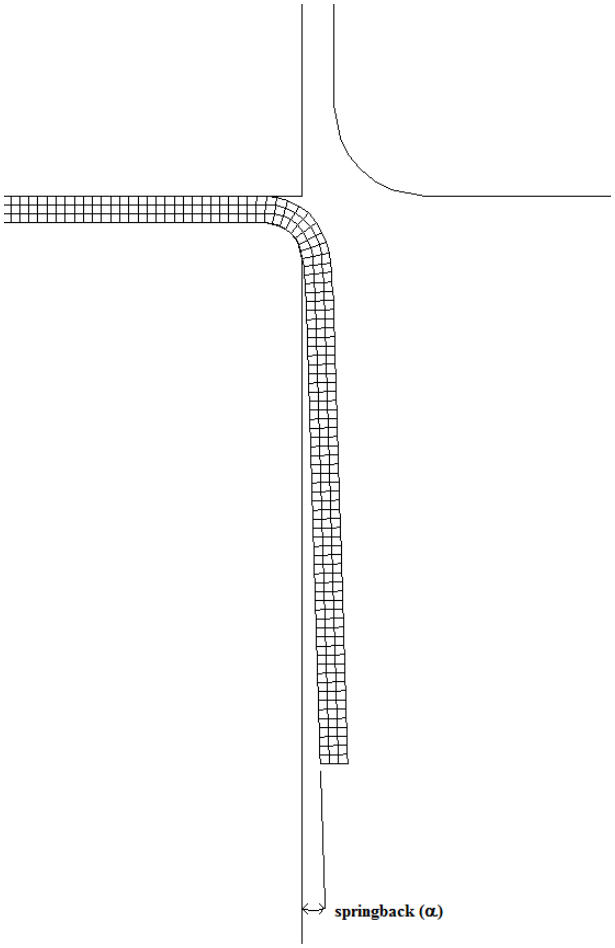

Figure 5.15 Springback angle in wipe bending

Table 5.16 Wipe bending models and springback results

	Material	Thickness (mm)	Die radius (mm)	Springback (°)
Model 1	Steel 1	1.5	2	1.74
Model 2	Steel 1	1.5	4	2.12
Model 3	Steel 1	3	6	1.68
Model 4	Steel 2	1.5	6	3.41
Model 5	Steel 2	2	4	2.54
Model 6	Steel 2	3	2	2.00
Model 7	Steel 3	1.5	4	2.70
Model 8	Steel 3	2	2	2.29
Model 9	Steel 3	3	6	2.12
Model 10	Steel 4	2	2	2.56
Model 11	Steel 4	2	6	2.91
Model 12	Steel 4	3	4	2.18

Different combinations of die radius, thickness, and material are constructed in Table 5.16 and effects of these parameters on springback are investigated for wipe bending process.

When model 1 and model 2 are compared it is observed that springback amounts increase as the die radius increases for the same material and same thickness. In a similar manner when model 3 and model 9 compared it is seen that springback amounts increase as yield strength of the material increases for the same thickness and same die radius. When model 6 and model 10 are compared springback amounts decrease as thickness increases for nearly the same yield strength and same die radius. The dominant parameter for springback phenomenon seems to be thickness among these parameters.

To investigate effects of thickness, die radius, and yield strength on von Mises stress Table 5.17 constructed.

Table 5.17 Maximum von Mises stress results

	Thickness (mm)	**Die radius (mm)**	**Yield strength (MPa)**	**Max. von Misses stress (fully loaded) (MPa)**	**Max. von Misses residual stress (unloaded) (MPa)**
Model 1	1.5	2	185	322.8	218.4
Model 2	1.5	4	185	301.6	192.4
Model 3	3	6	185	354.4	295.7
Model 6	3	2	325	701.6	422.2
Model 9	3	6	286	423.7	266.6
Model 10	2	2	340	523.5	332.8

When model 1 and model 2 are compared it is seen that maximum von Mises stress decreases a bit as die radius increases for the same material and same thickness. When model 3 and model 9 are compared it is found that material with higher yield strength exhibits much higher maximum von Mises stress values than the material with lower yield strength for the same thickness and same die radius. When model 6 and model 10 are compared it is observed that maximum von Mises stress increases excessively as thickness increases for the same die radius and nearly the same yield strength. Also, there is an important drop in the value of the maximum von Mises stress values after the backing of the punch for all operations.

In addition to the aforementioned maximum von Mises stress values, other types of stress distributions are also investigated. In Figures 5.16 and 5.17 von Mises stress distributions in steel 4 for 2-mm-thick sheet with 6 mm die radius is illustrated.

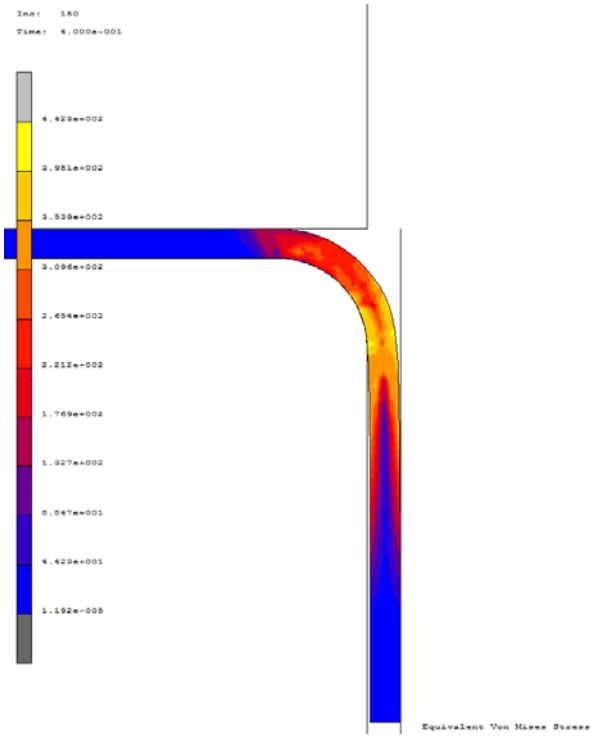

Figure 5.16 Von Mises stress distribution in steel 4 for 2-mm-thick sheet with 6 mm die radius at fully loaded stage

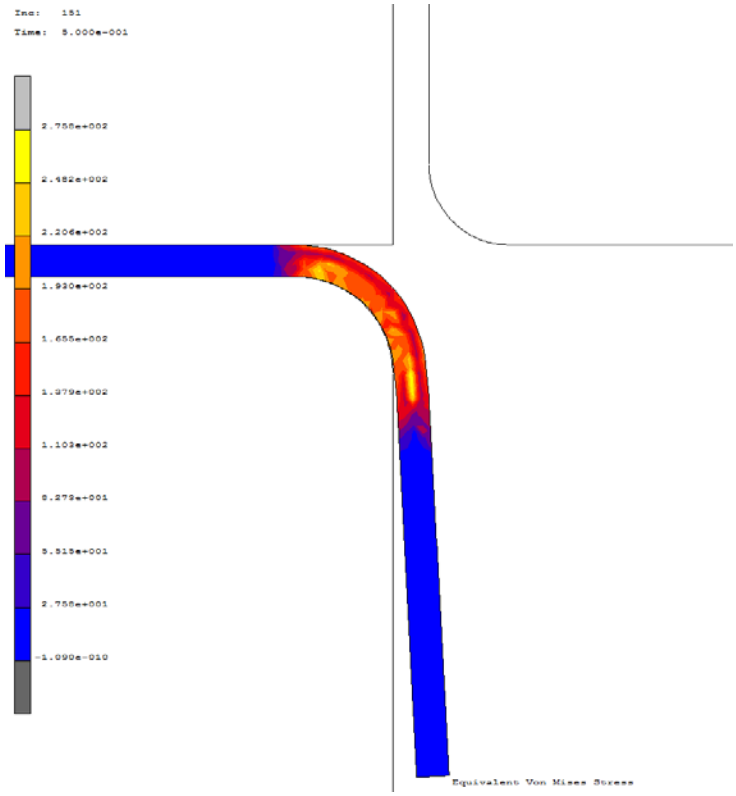

Figure 5.17 Residual von Mises stress distribution in steel 4 for 2-mm-thick sheet with 6 mm die radius at unloaded stage

In Figures 5.18 and 5.19, normal stresses in longitudinal direction in steel 1 for 1.5-mm-thick sheet with 4 mm die radius are illustrated.

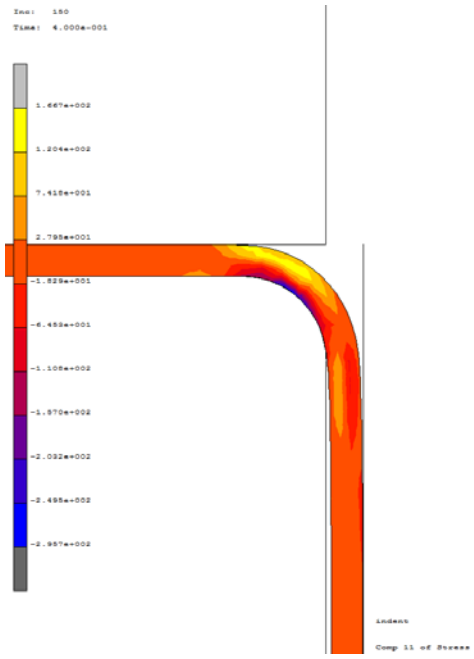

Figure 5.18 Normal stress distribution in longitudinal direction in steel 1 for 1.5-mm-thick sheet with 4 mm die radius at the fully loaded stage

Figure 5.19 Residual normal stress distribution in longitudinal direction in steel 1 for 1.5-mm-thick sheet with 4 mm die radius at the unloaded stage

Figures 5.18 and 5.19 show that at the fully loaded stage, normal stresses along the longitudinal direction and the residual stresses distribution in the unloaded stage appeared. Figures 5.16 and 5.17 verify the expected stress distribution as localized in the bent-up region in bending process.

5.3.2 ANN Development of Wipe Bending

In this case study, two different training data sets and two different testing data sets for wipe bending process are crated. Created training data sets are shown in Table 5.18 and Table 5.19. In the first training data set, models 1-5, 7-10, and 12 are used. Model 6 and model 11 are used for testing part. In the second training data set, models 1, 3-7, and 9-12 are used. Model 2 and model 8 are used for testing part. Constructed testing data sets are shown in Table 5.20 and Table 5.21.

Table 5.18 First training data set

	Thickness (mm)	**Die radius (mm)**	**K (MPa)**	**n**	**Springback (°)**
Model 1	1.5	2	635	0.25	1.74
Model 2	1.5	4	635	0.25	2.12
Model 3	3	6	635	0.25	1.68
Model 4	1.5	6	683	0.17	3.41
Model 5	2	4	683	0.17	2.54
Model 7	1.5	4	721	0.33	2.70
Model 8	2	2	721	0.33	2.29
Model 9	3	6	721	0.33	2.12
Model 10	2	2	754	0.21	2.56
Model 12	3	4	754	0.21	2.18

Table 5.19 Second training data set

	Thickness (mm)	**Die radius (mm)**	**K (MPa)**	**n**	**Springback (°)**
Model 1	1.5	2	635	0.25	1.74
Model 3	3	6	635	0.25	1.68
Model 4	1.5	6	683	0.17	3.41
Model 5	2	4	683	0.17	2.54
Model 6	3	2	683	0.17	2.00
Model 7	1.5	4	721	0.33	2.70
Model 9	3	6	721	0.33	2.12
Model 10	2	2	754	0.21	2.56
Model 11	2	6	754	0.21	2.91
Model 12	3	4	754	0.21	2.18

Table 5.20 First testing data set

	Thickness (mm)	Die radius (mm)	K (Mpa)	n	Springback (°)
Model 6	3	2	683	0.17	2.00
Model 11	2	6	754	0.21	2.91

Table 5.21 Second testing data set

	Thickness (mm)	Die radius (mm)	K (Mpa)	n	Springback (°)
Model 2	1.5	4	635	0.25	2.12
Model 8	2	2	721	0.33	2.29

Springback depends on four independent parameters in each ANN system for wipe bending process as thickness, die radius, strength coefficient, and straining hardening exponent. Constructed ANN systems combine these four different parameters and try to draw a general pattern to achieve the final springback amount.

To investigate repeatability and accuracy of different ANN systems for the same database, two different data sets and two different testing data sets are created and used in training part. Different hidden layer numbers, different training and testing percentages are tried and best results are achieved with eight hidden layers and seven hidden layers for the first and second training sets respectively. Results are shown in Table 5.22 and Table 5.23.

Table 5.22 ANN results for the first system

8 Hidden Layers					
	Thickness (mm)	**Die radius (mm)**	**K (MPa)**	**n**	**Springback (°)**
Model 6	3	2	683	0.17	1.98
Model 11	2	6	754	0.21	2.88

Table 5.23 ANN results for the second system

7 Hidden Layers					
	Thickness (mm)	**Die radius (mm)**	**K (MPa)**	**n**	**Springback (°)**
Model 2	1.5	4	635	0.25	2.13
Model 8	2	2	721	0.33	2.36

Obtained ANN results are compared with the testing data, which are FEA results, and relative percent errors are calculated, as given in Table 5.24.

Table 5.24 Relative errors in percentage

					Springback (°)		
	Thickness (mm)	**Die radius (mm)**	**K (Mpa)**	**n**	**FEA**	**8 Hidden Layers**	**Error (%)**
Model 6	3	2	683	0.17	2.00	1.98	1.00
Model 11	2	6	754	0.21	2.91	2.88	1.03

					Springback (°)		
	Thickness (mm)	**Die radius (mm)**	**K (Mpa)**	**n**	**FEA**	**7 Hidden Layers**	**Error (%)**
Model 2	1.5	4	635	0.25	2.12	2.13	0.47
Model 8	2	2	721	0.33	2.29	2.36	3.05

Table 5.24 shows that both ANN systems predict springback effectively. In the first system, percentage errors are less than 1.03, it means that ANN system gave nearly same results with FEA. In the second system, percentage errors are between 0.47 and 3.05. From Table 5.24, it is seen that different training sets can be used for similar testing sets in the same database of springback results. These results verify repeatability and accuracy of different ANN systems for same database.

5.4 Industrial Workpiece

The developed approach aims to combine FEA/ANN so that bending operations of an industrial workpiece can be modeled, composed of air, V-die, and wipe bending processes. This industrial workpiece is used in a rotating part of military device.

The workpiece is produced by conventional machining techniques. This study combines three bending operations with the help of ANN and shows that this workpiece can be produced by bending operations without waste of material and time, resulting in a superior part when compared to the machined original. ANN results from other sections in Chapter 5 are employed for this purpose. These results are combined for the production steps of the complex shaped workpiece. The engineering drawings of the workpiece are given in Figures 5.20 and 5.21.

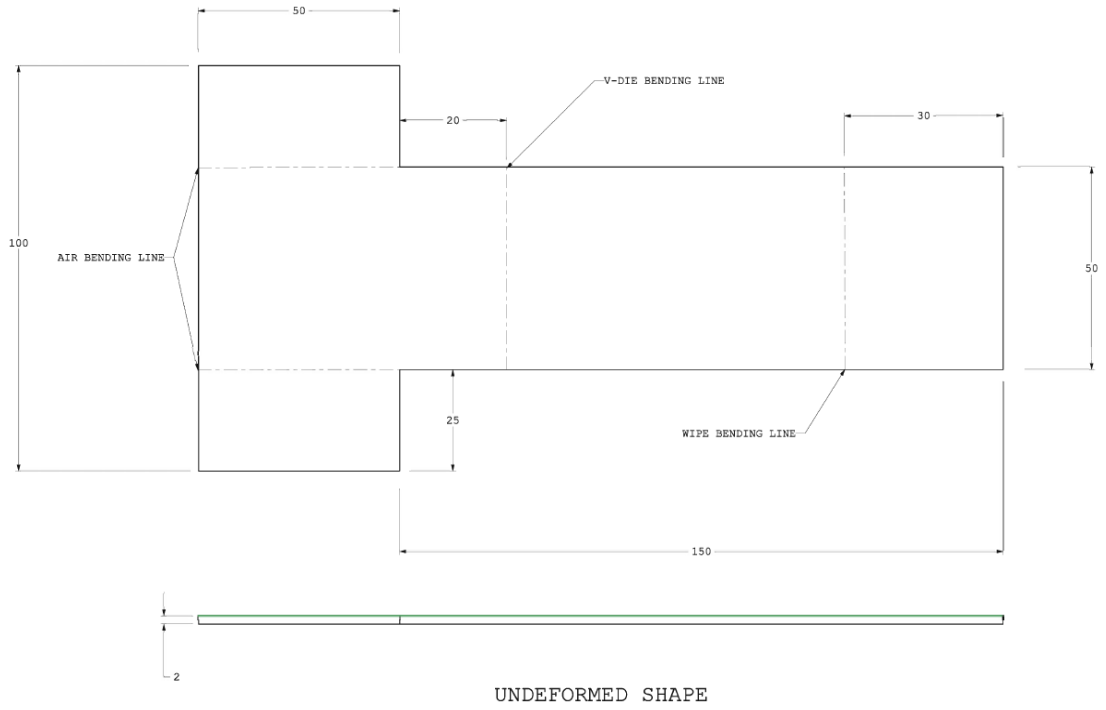

Figure 5.20 Schematic view of undeformed shape

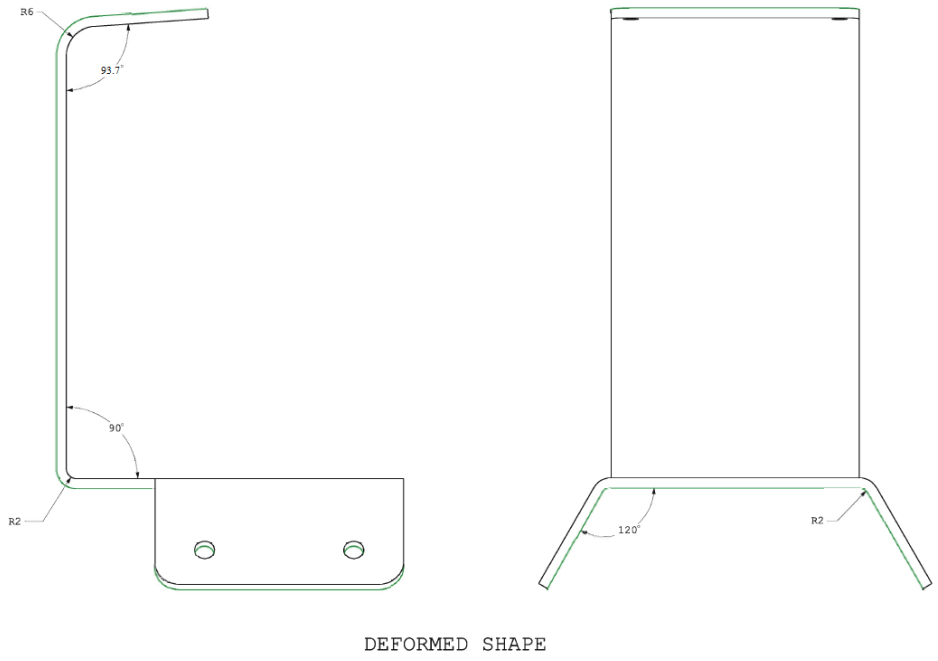

Figure 5.21 Schematic view of deformed shape

Material of the workpiece is SS304. Production stages are analyzed in three sections; namely, air bending, V-die bending, and wipe bending stages. Bending zones are illustrated in Figure 5.22.

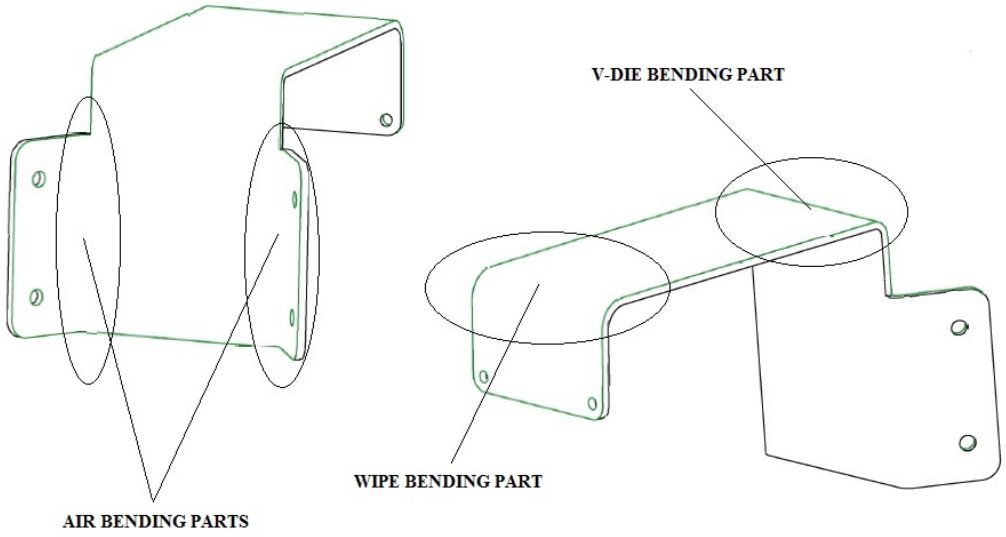

Figure 5.22 Localized parts of the operations

First operation on the workpiece is air bending. For air bending, ANN springback results of the section 5.1.2 are used. Two successive air bending operations with 120° are required. For this industrial piece ± 0.5° angle springback tolerances are assigned for the part acceptance thus acceptable bending angle is between 119.5 - 120.5°. Thickness of the workpiece is 2 mm. Radius of the bending side is 2 mm and dimensions of the workpiece are 50×50 mm. These parameters are appropriate to use section 5.1.2 results. Section 5.1.2 gives springback predictions for one side of the operations thus springback predictions are multiplied by 2. From Table 5.2 springback results are between 1.5 and 3° approximately. Total springback is between 3 and 6 ° approximately. To achieve 120° total angle, 116° bending angle is preferred. From Table 5.8 and Table 5.9, it is seen that model 8 is appropriate for springback prediction of this operation. Table 5.8 gives 1.90° springback prediction with 10 hidden layers and 1.06 percentage error. Total springback angle is 1.90×2=3.80°, thus achieved total angle after bending is 116+3.80=119.80° and this result is between required tolerance range which is 119.5-120.5°. This result shows once the ANN is developed, springback angle can be predicted with the help of ANN without the finite element analysis.

Second operation on the workpiece is V-die bending. For V-die bending side, ANN springback results of the section 5.2.2 are used. One V-die bending operation with 90° is

required. Again ± 0.5° angle springback tolerances are assumed to be acceptable, and thus bending angle must be between 90.5 and 89.5°. Thickness is 2 mm, radius of the bending side is 2 mm and dimensions of the workpiece are 140×50 mm. Section 5.2.2 results are appropriate for these parameters. Section 5.2.2 gives springback predictions for one side of the operations thus springback predictions are multiplied by 2 again. From Table 5.12 springback results are between -0.70 and -2.01°. To achieve 90° total angle, 93.5° bending angle is preferred. From Table 5.14 and Table 5.15, it is seen that model 13 is appropriate for springback prediction of this operation. Table 5.15 gives -1.83° springback prediction with 5 hidden layers and 0.55 percentage error. Total springback angle is -1.83×2=-3.66°, thus achieved total angle after bending is 93.5-3.66=89.84° and this result is between required tolerance range which is 89.5-90.5°. This result shows that ANN results for extrapolations can be used effectively. Again if there is no extra FEA of this type of material and operation, springback angle can be predicted with the help of ANN development and this result can be used for prediction of springback by design engineers even for different bending angles.

Third and last operation on the workpiece is wipe bending. For wipe bending side, ANN springback results of the section 5.3.2 are used. One wipe bending operation with 93.7° part angle is required. ± 0.5° angle tolerances are assumed to be acceptable and thus bending angle must be between 93.2 and 94.2°. Thickness is 2 mm. Radius of the bending side is 6 mm and dimensions of the workpiece are 100×50 mm. Section 5.3.2 results are appropriate for these parameters. The angle is 93.7°. From Table 5.16 springback results are between 1.68 and 3.41°. To achieve 93.7° angle, bending of steel 4 with 2 mm preferred. From Table 5.22 and Table 5.24, it is seen that model 10 is appropriate for springback prediction of this operation. Table 5.24 gives 2.88° springback prediction with 8 hidden layers and 1.03 percent error. Thus the achieved angle after bending is 90+2.88=92.88°. There is also 0.25 mm clearance which required for wipe bending operation and this clearance causes 0.48° angle approximately which is shown in Figure 5.23. Total bending angle is completed with 92.88+0.48=93.36° and this result is between required tolerance range which is 93.20-94.20°. This result shows again that if there is no extra FEA of this type of material and operation, springback angle can be predicted with the help of ANN development and this result can be used for prediction of springback by design engineers without waste of time.

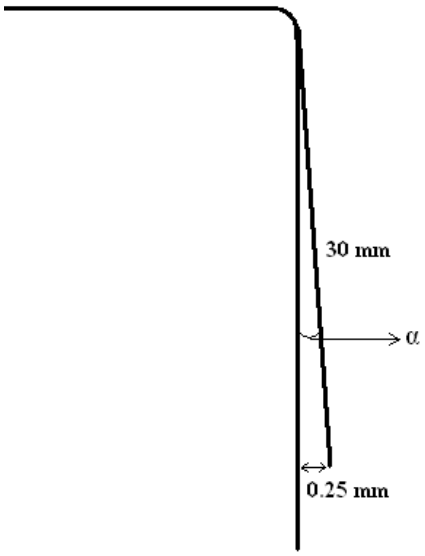

Figure 5.23 Angle due to clearance

There are holes on the wings of the workpiece which are used to fasten the workpiece onto the device (Figure 5.22). These holes can be drilled after bending operation, and by doing so, effects of drilling on sheet can be prevented. In addition, those holes are sufficiently far away from bending zones.

CHAPTER 6

EXPERIMENTS BASED ANN PLATFORM FOR AIR BENDING

In this chapter, firstly, experiments of the air bending processes are carried out and results of the experiments are compared with the results of FEA. Secondly, artificial neural network development based on experimental results is conducted. Unlike previous chapter, ANN is based on experimental results to show feasibility of ANN with experimentation. Experimentation is also used for validation of FEM of the process.

In the simulations, air bending operations are considered as plane strain. Four-node quadrilateral plane strain elements are used in FEA. Friction between sheet, punch, and die has been utilized by means of Coulomb's law, where the friction coefficient is taken as 0.05. In this study, steel sheets (SS 304) are assumed to be free of residual stresses before loading starts. Updated Lagrange procedure is preferred as an analysis option, which is employed in large strain and large displacement analyses. Multilayer feedforward backpropagation algorithm is used as ANN system algorithm.

6.1 FEA and Experimentation of Air Bending

In this case study, angular bending is modeled and simulated for eight different bending angles and two different sheet thicknesses. Sheet thicknesses are 1 and 1.5 mm. For 1 mm sheet thickness, bending angles are 93.6°, 101.4°, 112.3°, and 128.0°. For 1.5 mm sheet thickness, bending angles are 92.3°, 118.5°, 121.0°, and 134.0°. The experiments of the simulated cases are carried out in the Machine Shop of the office of General Workshops, METU, and the FEA results of springback are compared with the experimental springback results. The press used in the experiments is shown in Appendix A.

The dimensions of the punch and die used in bending are illustrated in Figure 6.1. The steel sheet is placed on the die, and the punch moves vertically downward towards to sheet until the desired angle is achieved. Additional figures on bending press machine are supplied in Appendix A.

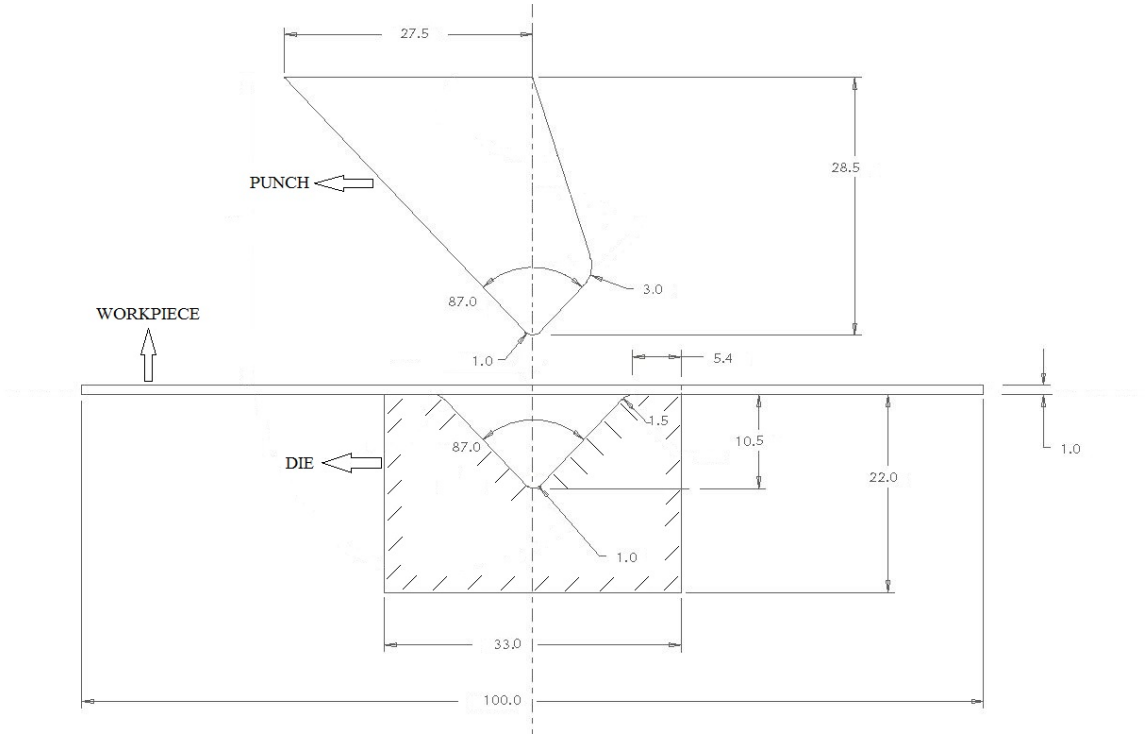

Figure 6.1 Schematic view of experimental setup

Plastic strain-true stress data is achieved by tension test as stated in Chapter 5. The tension test was carried out in the Materials Testing Laboratory of the Department of Mechanical Engineering, METU. The figures related to the tension tests are provided in Appendix B.

All steel sheets have the modulus of elasticity of 200 GPa and a Poisson's ratio of 0.3 and yield strength of 340 MPa. For elastic – plastic deformation behavior, plastic strain-true stress data are given in Table 6.1. The workpieces have the dimensions of 100×100 mm. Bending angles of sheets at fully loaded case are calculated with the help of digital angle measuring device (Appendix C) which has a sensitivity of 0.1 degree.

Table 6.1 Strain hardening data

Stainless Steel (SS304)	
Plastic Strain(mm/mm)	**True Stress(MPa)**
0	340
0.0513	410
0.0862	445
0.1040	467
0.1500	510
0.2000	550
0.2950	591
0.3560	610

Angles of sheets after bending (part angle) at unloaded case are calculated with the help of coordinate measuring machine (CMM) in Aselsan Inc. (Appendix C).

6.1.1 Air Bending of 1 mm Steel Sheet

In this case study, the results gathered from the FEA and the experiments are provided in Table 6.2.

Table 6.2 FEA and experiment results for 1 mm steel

		Part Angle (°)		Springback (°)	
Thickness (mm)	**Bending Angle (°)**	**FEA**	**Experiment**	**FEA**	**Experiment**
1	93.6	102.4	103.4	4.4	4.9
1	101.4	108.8	109.8	3.7	4.2
1	112.3	118.3	119.3	3.0	3.5
1	128.0	133.0	133.2	2.5	2.6

From Table 6.2, it is observed that springback amounts decrease as bending angle increases. Table 6.2 shows that the results of springback amount for air bending, the FEM results and the experimental results are close and in good agreement. This outcome supports the idea that FEM can be used to simulate bending operations.

In addition to springback results, stress distributions are also investigated. In Figures 6.2 and 6.3, von Mises stress distributions in 1-mm-thick sheet with 112.3° bending angle are illustrated.

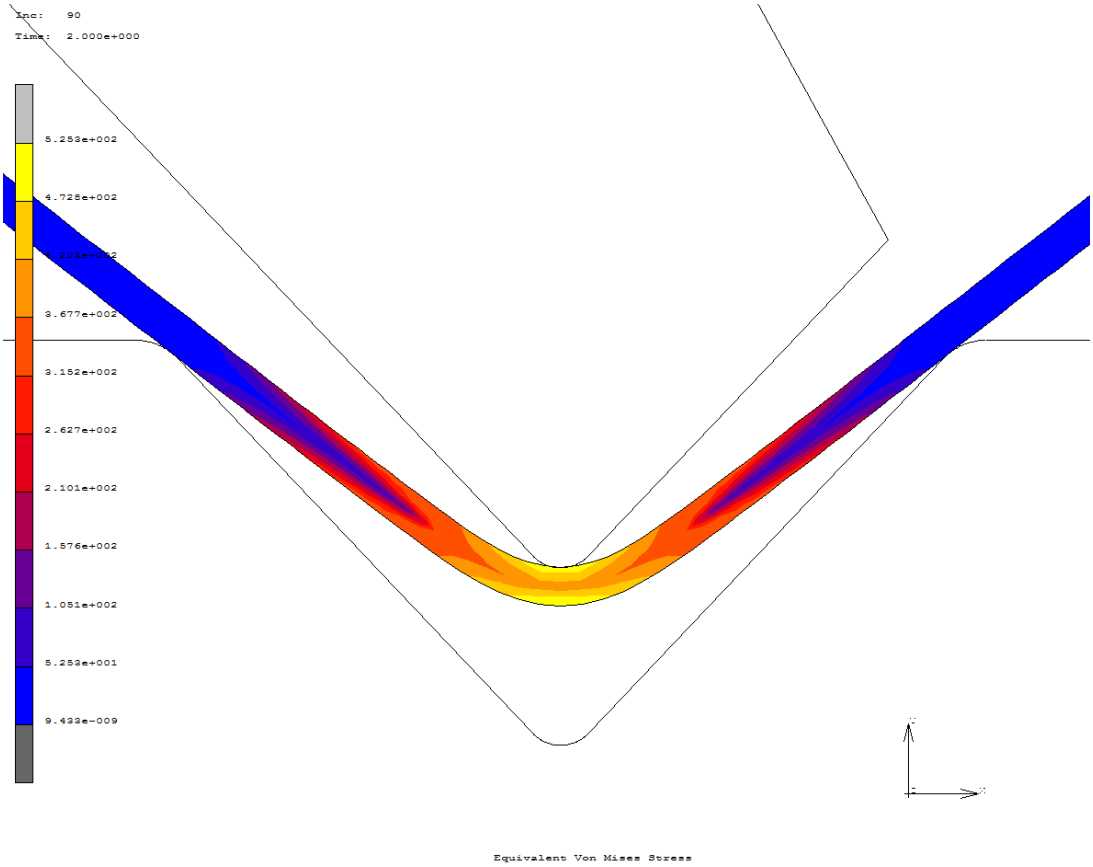

Figure 6.2 Von Mises stress distribution in 1-mm-thick sheet with 112.3° bending angle at fully loaded stage

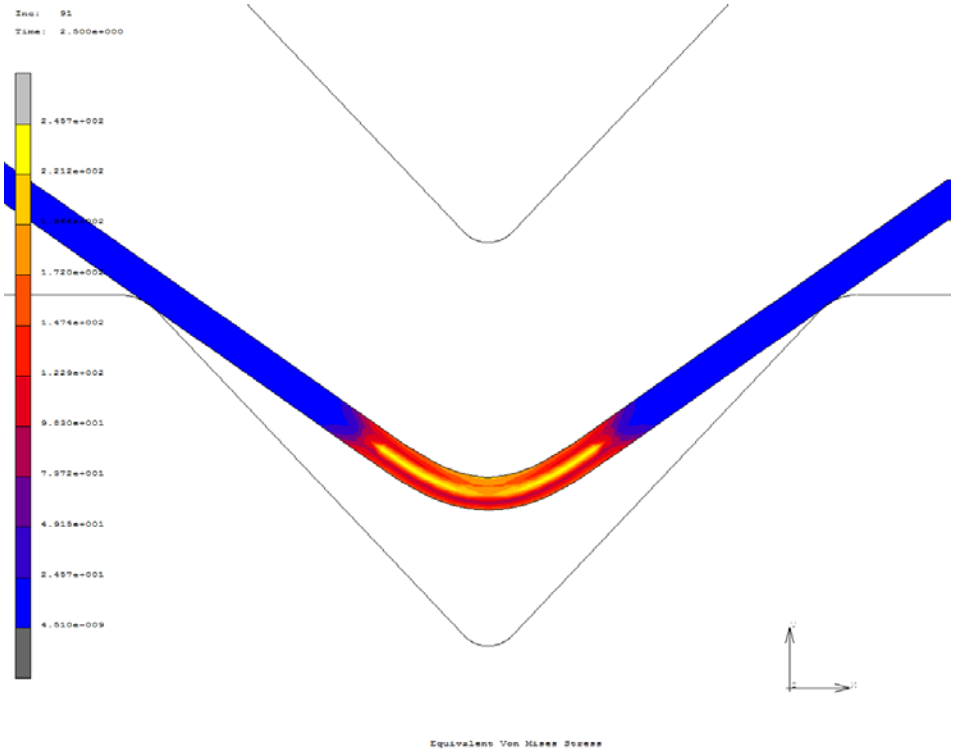

Figure 6.3 Von Mises stress distribution in 1-mm-thick sheet with 112.3° bending angle at unloaded stage

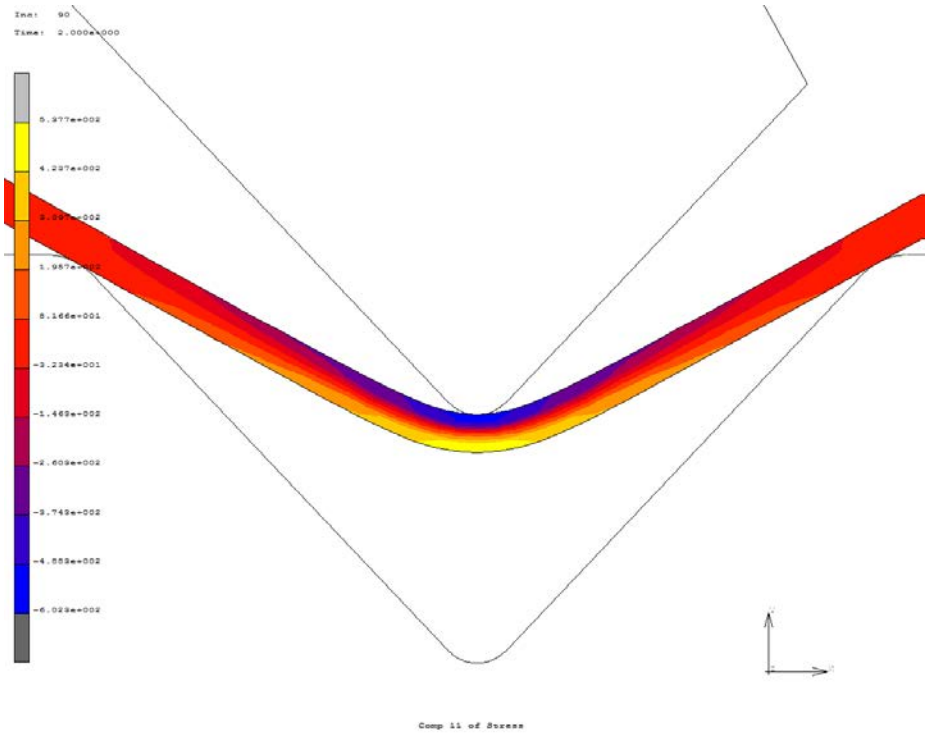

Figure 6.4 Normal stress distribution in longitudinal direction in 1-mm-thick sheet with 128.0° bending angle at the fully loaded stage

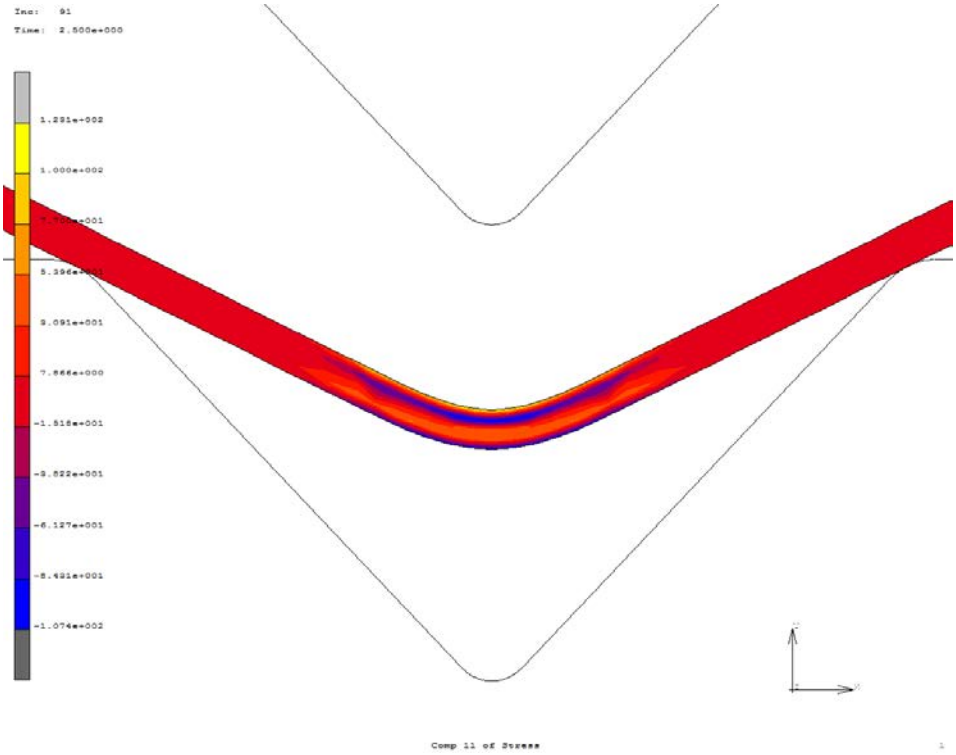

Figure 6.5 Normal stress distribution in longitudinal direction in 1-mm-thick sheet with 128.0° bending angle at the unloaded stage

In Figures 6.4 and 6.5, normal stresses in longitudinal direction in 1-mm-thick sheet with 128.0° bending angle are illustrated.

Figures 6.4 and 6.5 show that at the fully loaded stage, the middle regions of the sheet about the neutral axis are in elastic regime, while the inner and outer fibers are in the plastic regime. After unloading residual stresses appear and the distribution of the residual stresses are in agreement with theoretical information. Inside of the workpiece is under compression (inner fibers) while outside of the workpiece is in tension (outer fibers). Figures 6.2 and 6.3 show the von Mises stress distribution, which is localized in the bent-up region in bending process. Combination of these four stresses is highest at outer (inner and outer) fibers at the fully loaded stage and highest at the midst of the sheet at unloaded stage.

6.1.2 Air Bending of 2 mm Steel Sheet

In this case study, the results gathered from the FEA and the experiments are provided in Table 6.3.

Table 6.3 FEA and experiment results for 1.5 mm steel

		Part Angle (°)		Springback (°)	
Thickness (mm)	Bending Angle (°)	FEA	Experiment	FEA	Experiment
1.5	92.3	98.1	98.6	2.9	3.2
1.5	118.5	122.5	123.1	2.0	2.3
1.5	121.0	124.8	125.4	1.9	2.2
1.5	134.0	137.4	137.8	1.7	1.9

From Table 6.3, it is observed that springback amounts decrease as bending angle increases as expected. Table 6.3 shows that the results of springback amount for air bending, the FEM results and the experimental results are close and in good agreement. This outcome also supports the idea that bending operations can be simulated by FEM effectively.

In addition to springback results, stress distributions are investigated. Von Mises stress distributions in 1.5-mm-thick sheet with 134.0° bending angle are illustrated in Figures 6.6 and 6.7.

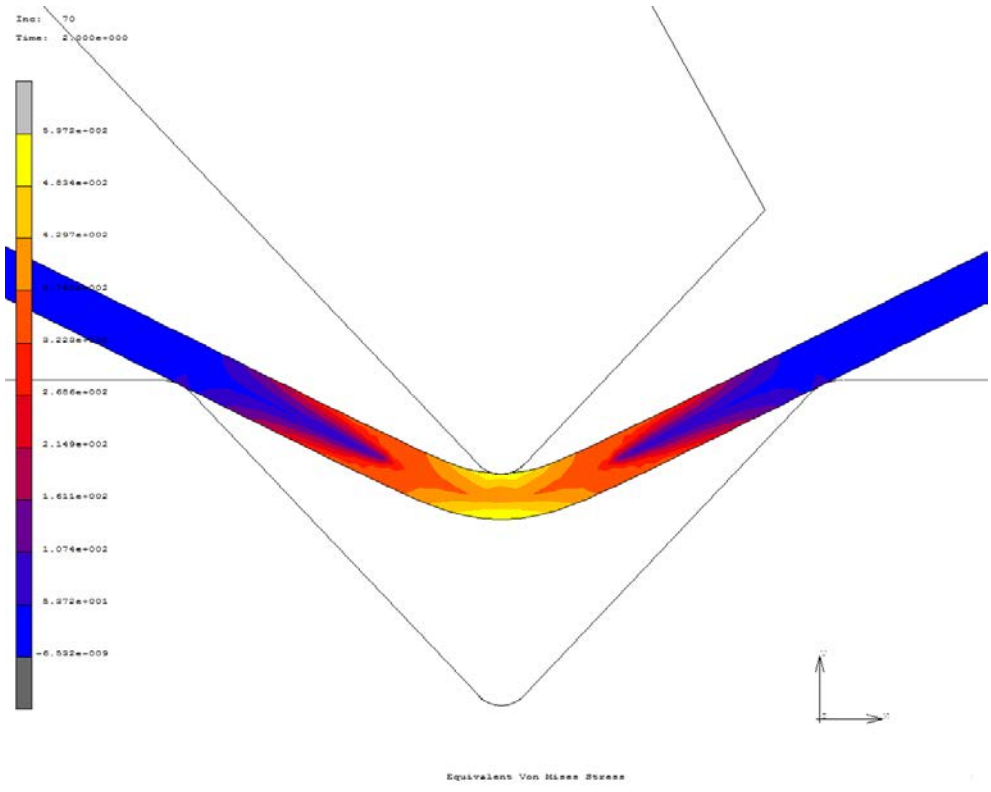

Figure 6.6 Von Mises stress distribution in 1.5-mm-thick sheet with 134.0° bending angle at fully loaded stage

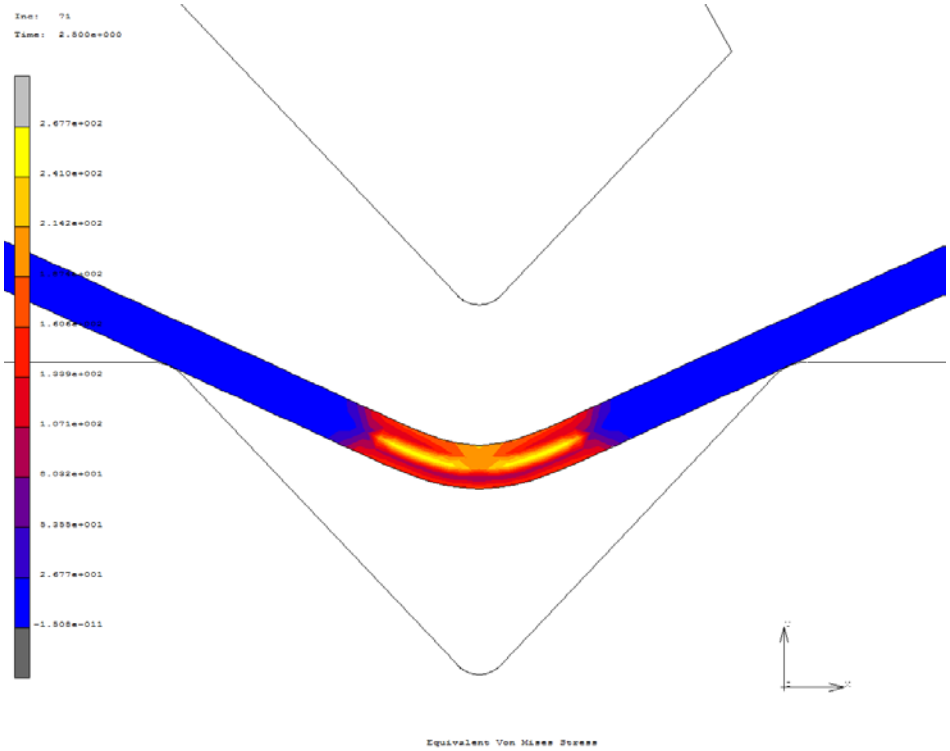

Figure 6.7 Von Mises stress distribution in 1.5-mm-thick sheet with 134.0° bending angle at fully loaded stage

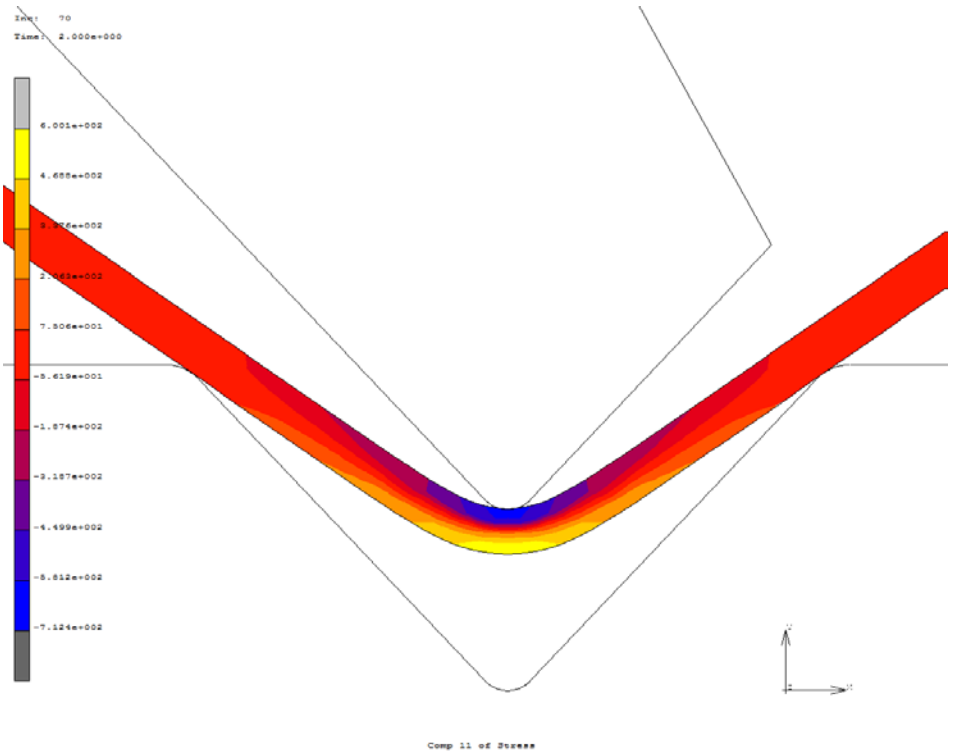

Figure 6.8 Normal stress distribution in longitudinal direction in 1.5-mm-thick sheet with 118.5° bending angle at the fully loaded stage

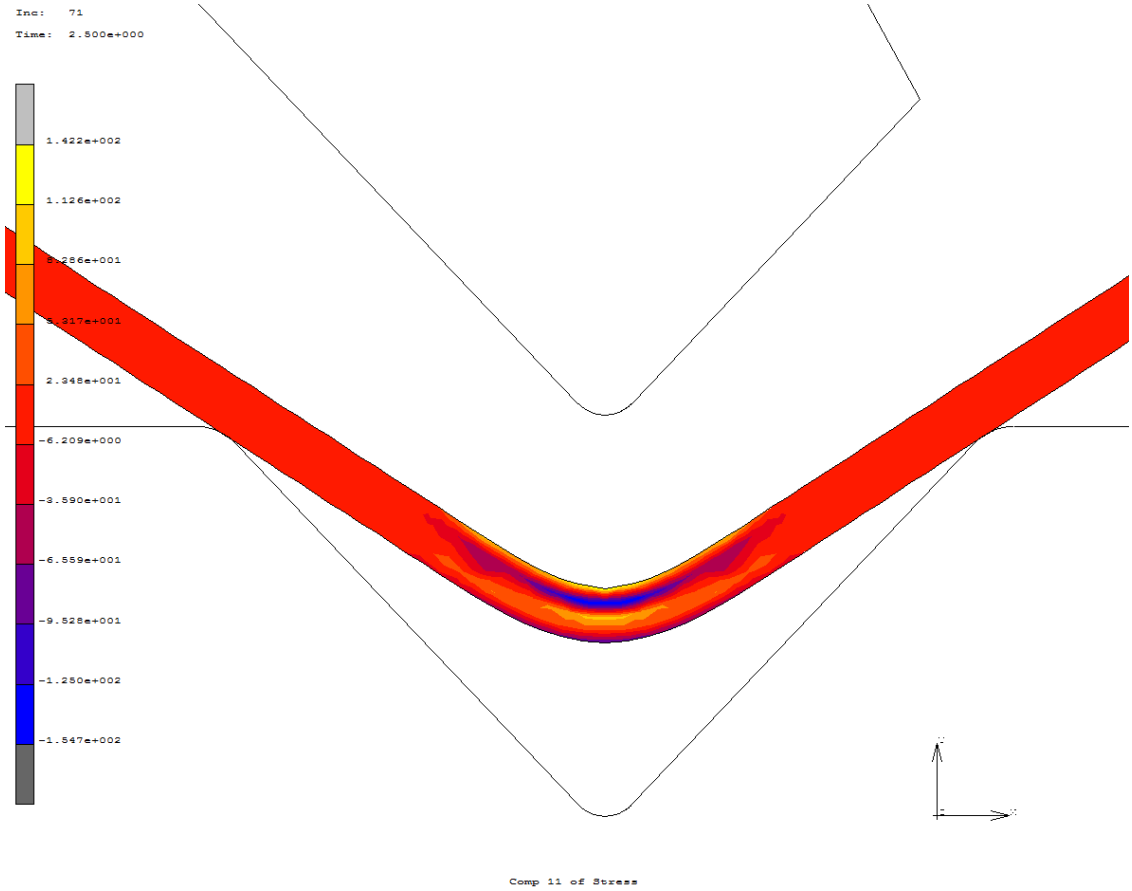

Figure 6.9 Normal stress distribution in longitudinal direction in 1.5-mm-thick sheet with 118.5° bending angle at the unloaded stage

Normal stresses in longitudinal direction in 1.5-mm-thick sheet with 118.5° bending angle are illustrated in Figures 6.8 and 6.9.

From Figures 6.8 and 6.9, it is observed that normal stresses along the longitudinal direction at the fully loaded stage, and the residual stresses distribution in the unloaded stage appear as expected. From Figures 6.6 and 6.7, it is seen that in the bent-up region shown with lighter color higher stress values are obtained as expected.

When Table 6.2 and Table 6.3 results are compared, it is seen that thickness of the workpiece has considerable affects on the springback results. Springback amounts decrease as thickness of the workpiece increases.

6.2 ANN Development of Experimental Air Bending Results

To predict springback amounts with ANN for air bending operations, an artificial neural network structure is developed which is based on experimental results. Three different training data sets and three different testing data sets for air bending process are created.

Training data sets are shown in Table 6.4, Table 6.5, and Table 6.6. Constructed testing data sets are shown in Table 6.7, Table 6.8, and Table 6.9.

Table 6.4 First training data set

Thickness (mm)	Bending Angle (°)	Springback (°)
1	93.6	4.9
1	112.3	3.5
1	128.0	2.6
1.5	92.3	3.2
1.5	121.0	2.2
1.5	134.0	1.9

Table 6.5 Second training data set

Thickness (mm)	Bending Angle (°)	Springback (°)
1	93.6	4.9
1	101.4	4.2
1	128.0	2.6
1.5	92.3	3.2
1.5	118.5	2.3
1.5	134.0	1.9

Table 6.6 Third training data set

Thickness (mm)	Bending Angle (°)	Springback (°)
1	93.6	4.9
1	112.3	3.5
1	128.0	2.6
1.5	92.3	3.2
1.5	118.5	2.3
1.5	121.0	2.2
1.5	134.0	1.9

Springback depends on two independent parameters in each ANN system for air bending process and these parameters are thickness and bending angle. Constructed ANN systems

combine these two different parameters and try to draw a general pattern to achieve the final springback amount.

Table 6.7 First testing data set

Thickness (mm)	Bending Angle (°)	Springback (°)
1	101.4	4.2
1.5	118.5	2.3

Table 6.8 Second testing data set

Thickness (mm)	Bending Angle (°)	Springback (°)
1	112.3	3.5
1.5	121.0	2.2

Table 6.9 Third testing data set

Thickness (mm)	Bending Angle (°)	Springback (°)
1	101.4	4.2

To investigate repeatability, accuracy and robustness of different ANN systems for the same database, three different training data sets and three different testing data sets are created and used in training part. Different hidden layer numbers, different training and testing percentages are tried and results are achieved. Results are shown in Table 6.10, Table 6.11, and Table 6.12.

Table 6.10 ANN results for the first system

4 Hidden Layers		
Thickness (mm)	Bending Angle (°)	Springback (°)
1	101.4	4.10
1.5	118.5	2.34

Table 6.11 ANN results for the second system

4 Hidden Layers		
Thickness (mm)	**Bending Angle (°)**	**Springback (°)**
1	112.3	3.33
1.5	121.0	2.25

Table 6.12 ANN results for the third system

3 Hidden Layers		
Thickness (mm)	**Bending Angle (°)**	**Springback (°)**
1	101.4	4.18

Obtained ANN results are compared with experimental results, and relative percent errors are calculated, as given in Table 6.13.

Table 6.13 Relative errors in percentage

First System				
		Springback (°)		
Thickness (mm)	**Bending Angle (°)**	**Experiment**	**NN (4 Hidden Layers)**	**Error (%)**
1	101.4	4.20	4.10	2.38
1.5	118.5	2.30	2.34	1.74

Second System				
		Springback (°)		
Thickness (mm)	**Bending Angle (°)**	**Experiment**	**NN (4 Hidden Layers)**	**Error (%)**
1	112.3	3.50	3.33	4.86
1.5	121.0	2.20	2.25	2.27

Third System				
		Springback (°)		
Thickness (mm)	**Bending Angle (°)**	**Experiment**	**NN (3 Hidden Layers)**	**Error (%)**
1	101.4	4.20	4.18	0.48

Table 6.13 clearly shows that the constructed ANN systems with the selected parameters are highly capable of predicting the springback amounts for the air bending process. The percentage error is between 0.48 and 4.86. It is observed that if the number of training input increases (Table 6.9), ANN system requires less hidden layers and converges quickly. Accuracy of the ANN system's result increases with increasing training input/testing input ratio as in third system in Table 6.13. Error of third system is less than errors of both first and second systems.

From Table 6.13, it is seen that different training sets with the same size (first and second systems) can be used for similar testing sets in the same database of springback results. Percentage errors of these two systems are close to each other. These results verify repeatability and accuracy of different ANN systems for the same database.

Table 6.13 emphasizes that developed ANN systems are feasible and robust. All three ANN systems give very close results for springback predictions of air bending models. Table 6.13 also shows that if the number of independent parameters in the system decreases, system converges to desired outputs more quickly.

CHAPTER 7

CONCLUSION

7.1 Conclusions

In this study, the main aim is to determine the springback and to predict the final part shape in sheet metal forming operations by the use of ANN algorithms with FEA and experiments. Springback determination of air, V-die, and wipe bending operations are accomplished by the developed computational platforms. Several bending operations are analyzed and the amounts of springback are determined in order to overcome possible manufacturing problems. Also, steel sheets with two different thicknesses; 1, and 1.5 mm are used in the finite element simulations and artificial neural network system based on experimental data for air bendingprocess. The following conclusions can be drawn from the study:

- Constructed ANN systems with the selected parameters are highly capable of predicting the final part shapes for air, V-die, and wipe bending processes after springback. Constructed ANN systems predict springback amounts accurately.

- Accuracy of the ANN system result increases with increasing training input/testing input ratio as observed from the case study of V-die bending and experiments of air bending.

- The system should also not be over trained. This can be decided during the ANN development process by trial-and-error sensitivity perturbation procedures.

- If the number of independent parameters in the system decreases, system converges to desired outputs rapidly. Hence, if the number of independent parameters in a system is high, an adequate number of FEA simulations or experiments should be carried out to get accurate results.

- Developed ANN results of V-die bending sections shows that ANN systems can be used for extrapolations to predict springback. For accurate extrapolations, training inputs for the ANN system should be robust in itself and training set size should be large enough.

- As observed from the case study of wipe bending, different training sets can be used for similar testing sets in the same database of springback results. These results verify the repeatability and accuracy of different ANN systems for the same database.

- Die radius and punch radius variations in air bending do not significantly affect springback amount. Since sheet touches the die and punch through a line thus bending not affected from die radius changes considerably.

- It is seen that from all of the case studies, the material with higher yield strength exhibits much higher von Mises stress values than the material with lower yield strength. Also, a significant drop occurs in the value of the maximum von Mises stress values after the backing of the punch for all applications as observed from residual stress distributions.

- Two different bent-up regions exist in V-die bending process; namely, primary and secondary. These regions cause springback in opposite directions. Negative springback results (springforward) are obtained in this study due to the dominant elastic recovery of the secondary bent-up regions.

- It is observed that from all of the case studies, at the fully loaded stage, the core of the sheet is in elastic regime, while the outer fibers are in the plastic regime. After unloading residual stresses appear and the distribution of the residual stresses are in agreement with theoretical information. The expected stress distribution is localized in the bent-up region in bending processes.

7.2 Future Recommendations

For future work, the followings could be considered:

- Different bending operations such as angular bending, hemming, U-bending may be analyzed in FEA and ANN aspects.

- Effects of the different parameters such as different materials, and bend angles on springback amount in different bending operations may be investigated.

- FEA with ANN system may be used in conjunction with optimization. Automated analyses results may be achieved for a wide range of specific operations.

REFERENCES

1. IE 337: Materials and Manufacturing in Metal Forming: Bending. March 3 2010. p. 1-4.

2. Esat, V., 2002, Finite element analysis of springback in bending process, MSc thesis, Middle East Technical University, Ankara, Turkey. .

3. Schuler, Basic principles of metal forming, in Metal Forming Handbook C.e.P.T. Altan, Editor. 1998, Springer-Verlag: Göppingen.

4. Schmid, K., Manufacturing Processes for Engineering Materials 5th ed. 2008: Pearson Education.

5. Kazan, R., M. Fırat, and A.E. Tiryaki, Prediction of springback in wipe-bending process of sheet metal using neural network. Materials & Design, 2009. 30(2): p. 418-423.

6. Fu, Z., et al., Using genetic algorithm-back propagation neural network prediction and finite-element model simulation to optimize the process of multiple-step incremental air-bending forming of sheet metal. Materials & Design. 31(1): p. 267-277.

7. Wang, J., et al., Springback control of sheet metal air bending process. Journal of Manufacturing Processes, 2008. 10(1): p. 21-27.

8. Thipprakmas, S., Finite element analysis of punch height effect on V-bending angle. Materials & Design. 31(3): p. 1593-1598.

9. Tekiner, Z., An experimental study on the examination of springback of sheet metals with several thicknesses and properties in bending dies. Journal of Materials Processing Technology, 2004. 145(1): p. 109-117.

10. Groover, M.P., Fundamentals of Modern Manufacturing. Third ed. 2007.

11. Gardiner, A.G., 1957, The springback of metals, Trans ASME J Appl Mech, 79:1-9.

12. Panthi, S.K., et al., An analysis of springback in sheet metal bending using finite element method (FEM). Journal of Materials Processing Technology, 2007. 186(1-3): p. 120-124.

13. Lee, S.W. and D.Y. Yang, An assessment of numerical parameters influencing springback in explicit finite element analysis of sheet metal forming process. Journal of Materials Processing Technology, 1998. 80-81(0): p. 60-67.

14. Yi, H.K., Kim, D.W., Van Tyne, C.J., Moon, Y.H., 2008, Analytical prediction of springback based on residual differential strain during sheet metal bending, J Mech Eng Sci, 222:117-29.

15. I. Pahole, S. Bonifarti, M. Ficko, B. Vaupotic, S. Kovacic, J. Balic, Bending of sheet metal of complicated shapes (for 90º angle and more) in combined tools, Proceedings of the 11th International Scientific Conference "Contemporary

Achievements in Mechanics, Manufacturing and Material Science" CAM3S '2005, Gliwice - Zakopane, 2005, (CD-ROM).

16. Marretta, L., G. Ingarao, and R. Di Lorenzo, Design of sheet stamping operations to control springback and thinning: A multi-objective stochastic optimization approach. International Journal of Mechanical Sciences. 52(7): p. 914-927.

17. Hsu, T.-C. and I.-R. Shien, Finite element modeling of sheet forming process with bending effects. Journal of Materials Processing Technology, 1997. 63(1-3): p. 733-737.

18. Esat, V., H. Darendeliler, and M.I. Gokler, Finite element analysis of springback in bending of aluminium sheets. Materials & Design, 2002. 23(2): p. 223-229.

19. Meinders, T., et al., Numerical product design: Springback prediction, compensation and optimization. International Journal of Machine Tools and Manufacture, 2008. 48(5): p. 499-514.

20. Huang, Y.-M. and T.-C. Chen, An elasto-plastic finite-element analysis of sheet metal camber process. Journal of Materials Processing Technology, 2003. 140(1-3): p. 432-440.

21. Tekaslan, Özgür., U. Şeker, and A. Özdemir, Determining springback amount of steel sheet metal has 0.5 mm thickness in bending dies. Materials & Design, 2006. 27(3): p. 251-258.

22. Chan, W.M., et al., Finite element analysis of spring-back of V-bending sheet metal forming processes. Journal of Materials Processing Technology, 2004. 148(1): p. 15-24.

23. Nasrollahi, V. and B. Arezoo, Prediction of springback in sheet metal components with holes on the bending area, using experiments, finite element and neural networks. Materials & Design. 36(0): p. 331-336.

24. Song, N., Qian, D., Cao, J., Liu, W.K. and Li, S. (2001) `Effective prediction of springback in straight flanging', Journal of Engineering Materials and Technology, Vol. 123, No. 4, pp.456-461.

25. Ling, Y.E., H.P. Lee, and B.T. Cheok, Finite element analysis of springback in L-bending of sheet metal. Journal of Materials Processing Technology, 2005. 168(2): p. 296-302.

26. Supak Chanthapak, C.S., Sutasn Thipprakmas Influence of bottoming-bead geometry in wipe bending process TSME International Conference on Mechanical Engineering 2011.

27. de Vin, L.J., et al., A process model for air bending. Journal of Materials Processing Technology, 1996. 57(1-2): p. 48-54.

28. Zemin Fu, d.h., Xuhui Liu, Incremental air-bending forming simulation of sheet metal based on anisotropic plasticity theory. Optoelectronics and advanced materials – rapid communications, 2011. Vol. 5, No. 12: p. 1312 - 1319.

29. Garcia-Romeu, M.L., J. Ciurana, and I. Ferrer, Springback determination of sheet metals in an air bending process based on an experimental work. Journal of Materials Processing Technology, 2007. 191(1-3): p. 174-177.

30. Liu, W., et al., Springback prediction for sheet metal forming based on GA-ANN technology. Journal of Materials Processing Technology, 2007. 187-188(0): p. 227-231.

31. Ruffini R, Cao J. Using neural network for springback minimization in a channel forming process. J Mater Manuf 1998;107(5):65–73.

32. Inamdar, M.V., P.P. Date, and U.B. Desai, Studies on the prediction of springback in air vee bending of metallic sheets using an artificial neural network. Journal of Materials Processing Technology, 2000. 108(1): p. 45-54.

33. K. K. Pathak, S. Panthi, and N. Ramakrishnan, "Application of Neural Network in Sheet Metal Bending Process", Defence Science Journal, vol. 55, pp. 125-131, 2005.

34. Forcellese, A., F. Gabrielli, and R. Ruffini, Effect of the training set size on springback control by neural network in an air bending process. Journal of Materials Processing Technology, 1998. 80-81(0): p. 493-500.

35. Downes, A. and P. Hartley, Using an artificial neural network to assist roll design in cold roll-forming processes. Journal of Materials Processing Technology, 2006. 177(1-3): p. 319-322.

36. Cheng, P.J. and S.C. Lin, Using neural networks to predict bending angle of sheet metal formed by laser. International Journal of Machine Tools and Manufacture, 2000. 40(8): p. 1185-1197.

37. Viswanathan V, Kinsey B, Cao J (2003) Experimental implementation of neural network springback control for sheet metal forming. J Eng Mater Technol-Trans ASME 125(2):141–147.

38. Bak, M., "Cylindrical Bending of a Metal Plate with consideration of Temperature, and dynamic effects" 2003: Villneuve D'Ascq.

39. Bathe, K.-J., Introduction to Nonlinear Analysis, in Finite Element Procedures for Solids and Structures 1996, MIT Center for Advenced Engineering Study.

40. O.C. Zienkiewicz, R.L.T., Finite Element Modeling of contact phenomena in structural analysis. 6th ed. 2005: Elsevier Ltd.

41. Gershenson, C., Artificial Neural Networks for Beginners 2003.

42. Chakraborty, R., Fundamentals of Neural Networks. 2010.

43. Vincent Cheung, K.C., An Introduction to Neural Networks 2002.

44. Zilouchian, A., FUNDAMENTALS OF NEURAL NETWORKS in Intelligent Control Systems Using Soft Computing Methodologies 2001, CRC Press LLC.

45. Saumya Bajpai, K.J., and Neeti Jain, What is an artificial neural network?. International Journal of Soft Computing and Engineering (IJSCE), 2011. 1(NCAI2011).

46. Beale, H.D.M., Neuron Model and Network Architectures in Neural Network Toolbox 2000, The MathWorks.

47. M. I. A. Lourakis, "A brief description of the Levenberg-Marquardt algorithm implemented by levmar," http://www.ics.forth.gr/ lourakis/levmar/, February 11 2005.

48. Lee, M.-G., et al., Spring-back evaluation of automotive sheets based on isotropic-kinematic hardening laws and non-quadratic anisotropic yield functions, part III: applications. International Journal of Plasticity, 2005. 21(5): p. 915-953.

49. D. Kuhlman-Wilsdorf, Theory of plastic deformation - properties of low energy dislocation structures, Mat. Sci. Engn., A113 (1989) 1.

APPENDIX A

ADDITIONAL FIGURES ON AIR BENDING WITH A PRESS BENDING MACHINE

Figure A.1 Baykal bending press machine

Figure A.2 Baykal bending press machine

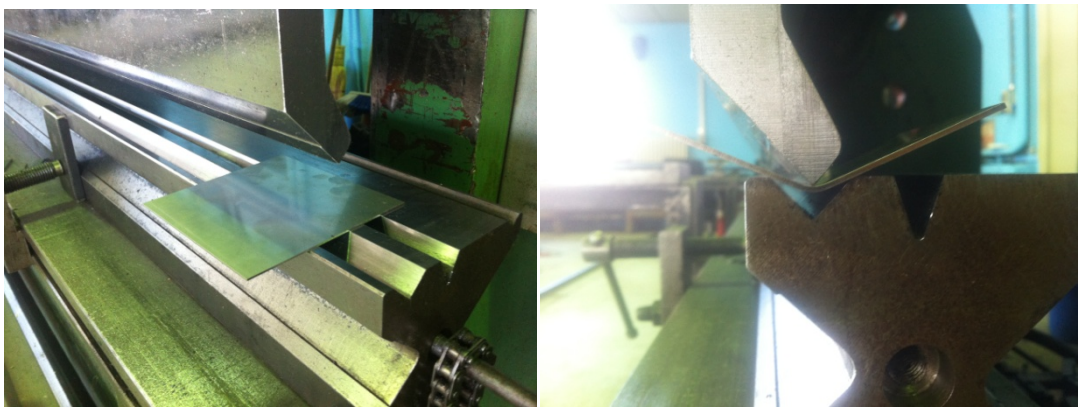

Figure A.3 Operational views of air bending

Figure A.4 1-mm-thick steel just before operation

Figure A.5 Calibration of bending press machine

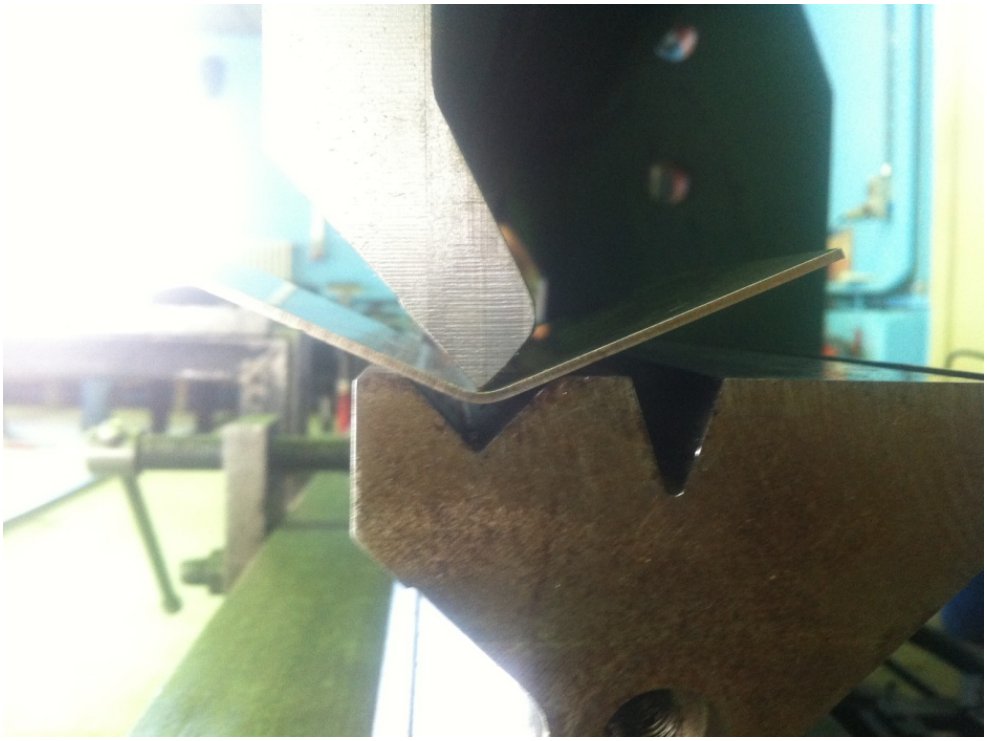

Figure A.6 1.5-mm-thick steel fully loaded stage

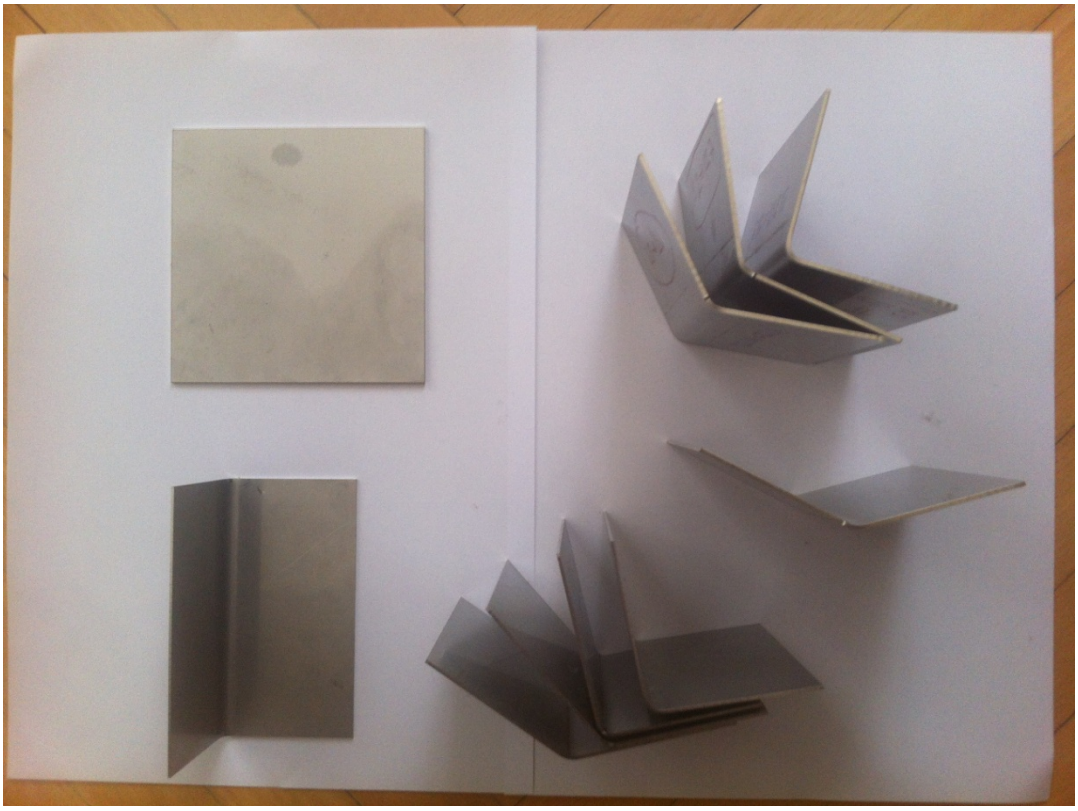

Figure A.7 Experimental sheets

APPENDIX B

FIGURES ON TENSION TESTS OF STEEL SHEETS

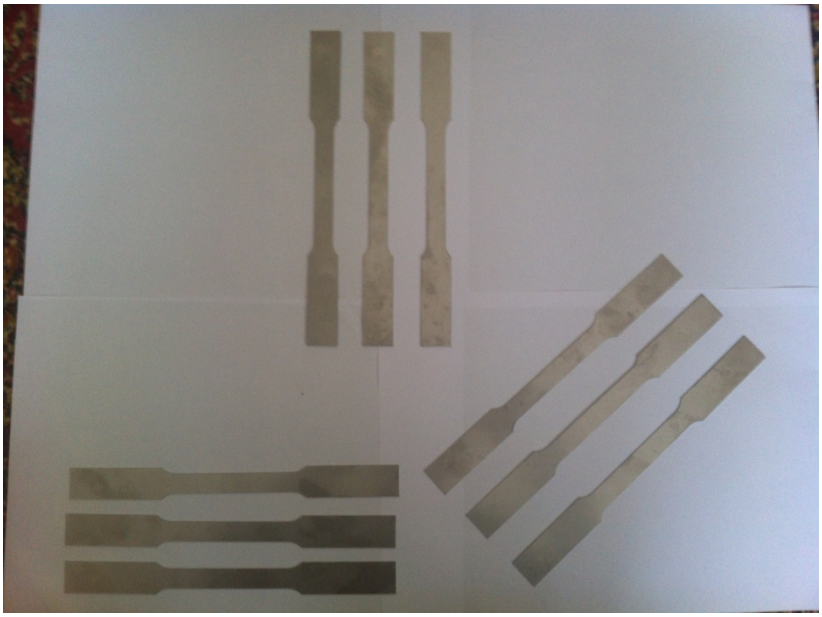

Figure B.1 1-mm-thick steels with angles of 0°, 45° and 90° with respect to the rolling direction before tension test

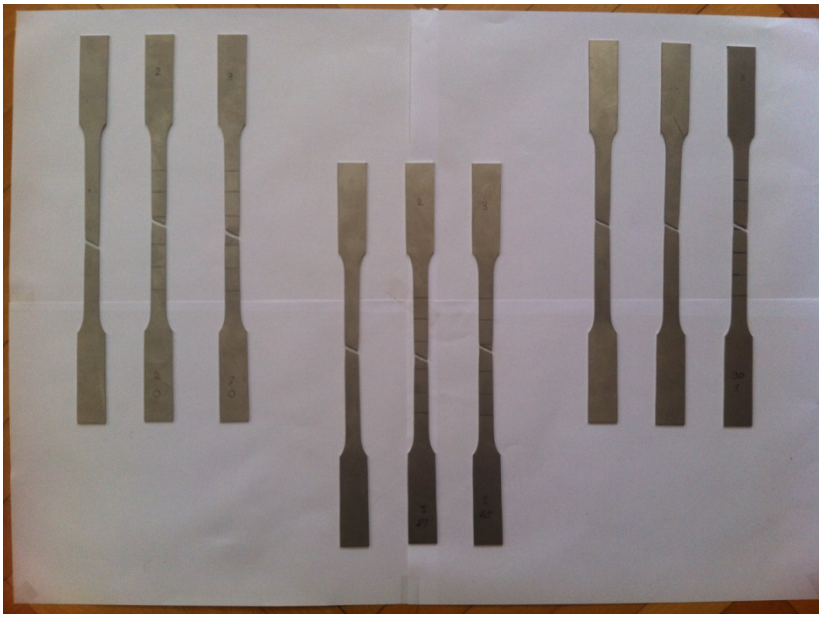

Figure B.2 1-mm-thick steels after tension test

APPENDIX C

FIGURES OF DIGITAL ANGLE MEASURING DEVICE AND CMM

Figure C.1 Digital angle measuring device

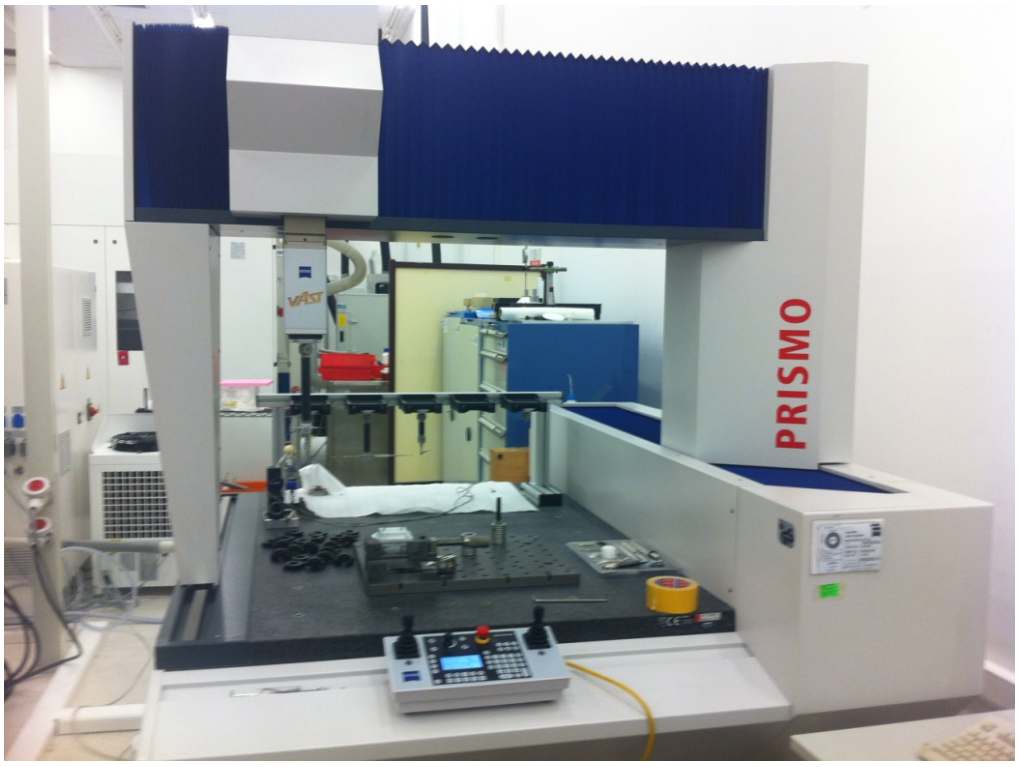

Figure C.2 CMM

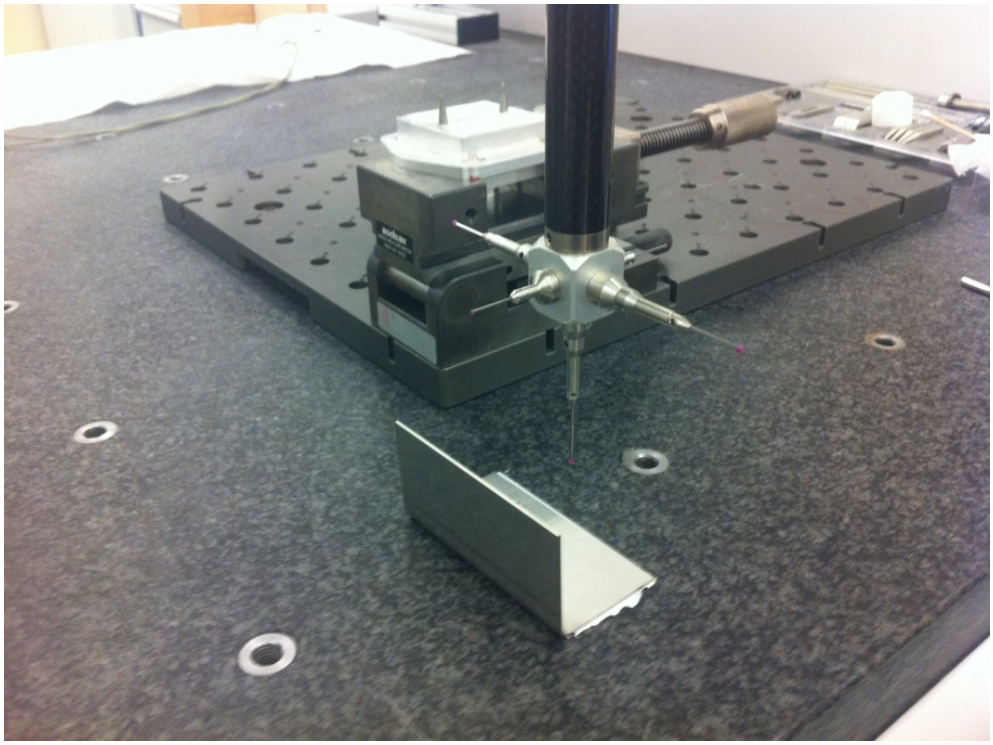

Figure C.3 Preparation of the measuring

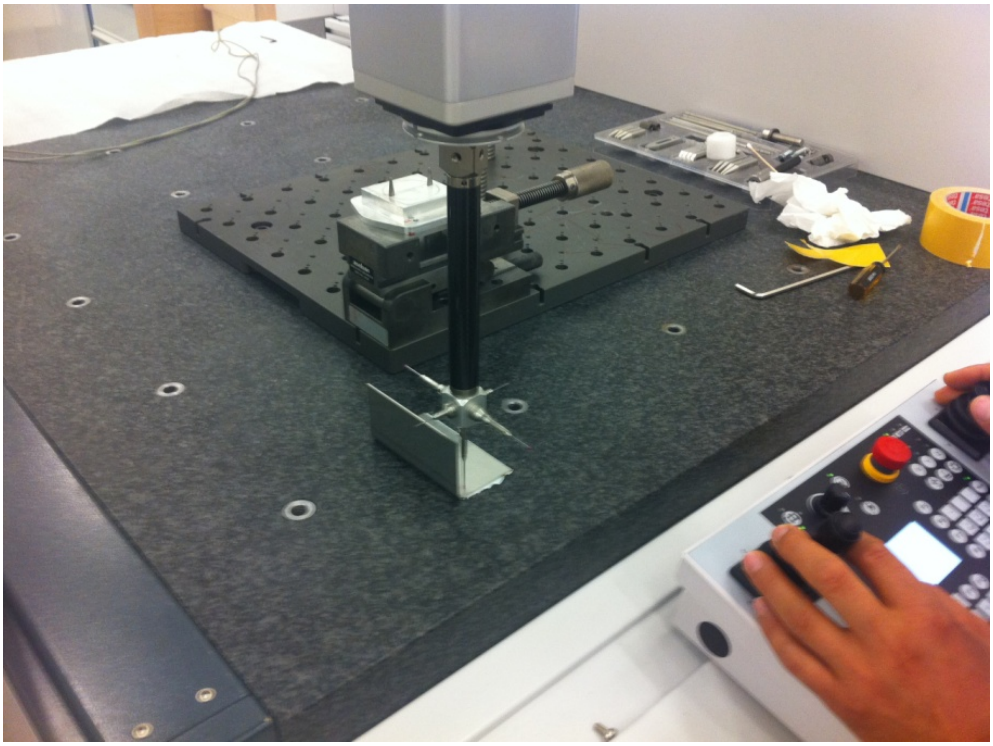

Figure C.4 While part angle measuring

Figure C.5 Monitoring results of part angle while measuring